

---

# Cretaceous mycelia preserving fungal polysaccharides: taphonomic and paleoecological potential of microorganisms preserved in fossil resins

---

M. SPERANZA<sup>1#</sup> C. ASCASO<sup>1</sup> X. DELCLÒS<sup>2</sup> E. PEÑALVER<sup>3,\*</sup>

<sup>1</sup>Departamento de Bioquímica y Ecología Microbiana, Museo Nacional de Ciencias Naturales  
Consejo Superior de Investigaciones Científicas, Serrano 115 bis, E-28006, Madrid, Spain.  
Speranza E-mail: speranzamariela@gmail.com Ascaso E-mail: ascaso@mncn.csic.es

<sup>2</sup>Departament d'Estratigrafia, Paleontologia i Geociències Marines, Universitat de Barcelona  
Martí i Franquès s/n, E-08028 Barcelona, Spain. E-mail: xdelclos@ub.edu

<sup>3</sup>Museo Geominero, Instituto Geológico y Minero de España  
Ríos Rosas 23, E-28003 Madrid, Spain. E-mail: e.penalver@igme.es

\* Corresponding author

# Current address: School of Applied Sciences, RMIT University, PO Box 71, Bundoora VIC 3083, Victoria, Australia

---

## ABSTRACT

---

The cortices of pieces of Cretaceous amber around the world commonly are constituted by networks of filamentous structures. Based on their morphological characteristics, such structures have previously been classified in different microorganismal groups. Their correct interpretation, however, is of great importance to establish the conditions of the resin's burial in the forest litter, and can provide important clues regarding the ecology and environmental conditions of Cretaceous resinous forests. Because these networks of filamentous structures present typical fungal morphological features we conducted a study in order to resolve their origin. The cortices of several pieces of Cretaceous amber from Spain were examined using light and scanning electron microscopy, energy dispersive X-ray spectroscopy and confocal laser scanning microscopy. This is the first time that Calcofluor white and Wheat germ agglutinin conjugated with fluorescein isothiocyanate have been employed as fungal markers in amber, and their use enabled us to detect preserved polysaccharides in the filamentous structures using confocal laser scanning microscopy. These results provide the first and oldest record of  $\beta$ -1,3 and  $\beta$ -1,4-linked polysaccharides, and specifically *N*-acetylglucosamine residues from chitin in a fossil fungus preserved in amber and to demonstrate that the networks of filamentous structures are mycelia composed of profuse hyphae of a resinicolous fungus. This type of mycelium constitutes one of the largest fungal fossil records known. Using taphonomic data it is demonstrated that the cortices originated during the Cretaceous due to fungal growth within non-solidified resin. The fossil diagenetic degradation sequence of the fungal hyphae and the surrounding amber is described. This degradation changed the microscopic appearance of the hyphae; thus, some of the previously indicated taxonomic features of this microorganism may actually be fossil diagenetic artifacts. The paleoecological implications with regard to fungal trophic requirements and forest environmental conditions are discussed.

---

**KEYWORDS** | Amber. Taphonomy. Paleoecology. Biomarkers. Fungi.

## INTRODUCTION

Amber provides clues regarding the origin and extinction of the flora and fauna of tropical and subtropical Mesozoic/Cenozoic forest ecosystems since the exceptional preservation of abundant small organisms -mainly arthropods- or their remains, sometimes various developmental stages of insects, prey and plant hosts, parasites and commensals, as well as exhibitions of defensive and social behavior (Martínez-Delclòs *et al.*, 2004; Arillo, 2007). Organisms that were trapped in resin, and are preserved in amber are called bioinclusions and some of them are especially informative about various taphonomic processes, paleoenvironmental conditions and important paleobiological aspects.

Most of the pieces of Cretaceous amber collected from outcrops in Spain have light brown, opaque cortices, which are present irrespective of the different color, size or shape of the pieces or any bioinclusion they may contain. The cortices of these Spanish pieces were first interpreted as degradation or alteration crusts (Alonso *et al.*, 2000; Peñalver *et al.*, 2007), mainly based on their high sulfur content revealed by an elemental analysis of samples from Álava (northern Spain) (Alonso *et al.*, 2000). Recently, Aquilina *et al.* (2013) reported that the cortices of Cretaceous amber pieces from southwestern France contain higher concentrations of Na and Ca cations, as well as some redox-sensitive trace elements such as Fe, than those found in the amber core.

Pieces of Cretaceous amber with cortices showing practically the same *de visu* features have been reported from other countries besides Spain, especially France (Breton, 2007; Girard *et al.*, 2009a). These have been studied by several authors using light and scanning electron microscopy (LM and SEM), and intricate assemblages of branched, filamentous structures with thick walls have been described (Breton, 2007; Beimforde and Schmidt, 2011). These peculiar fossils, not artifactual pseudofossils as chemical alterations of the amber, meet the criteria established by Waggoner (1994b) to separate microfossils from abiogenic pseudofossils in amber. Although a few networks of filamentous structures interpreted as fungal mycelia have been described in Cenozoic amber pieces, they show very different features (*e.g.*, Rikkinen and Poinar, 2000, 2001; Hower *et al.*, 2010).

Here an integrated study analyzing several cortices from various Spanish Cretaceous ambers using different microscopic techniques is reported. The features of both cortices and filamentous structures are ubiquitous in the Spanish amber pieces, which indicate that only one morphotype/taxon was implicated, although the presence of other taxa should not be ruled out. For the first time, two

specific stains widely used as fungal markers, CalcoFluor White (CFW) and Wheat Germ Agglutinin conjugated with Fluorescein Isothiocyanate (WGA-FITC), were employed to determine the nature of the networks of filamentous structures in amber cortices. The study reveals fungal origin of the abundant filamentous structures that constitute the cortices. In addition, it implicates new taphonomic and paleobiological data that increase our knowledge on exceptional preservation in amber.

## MATERIAL AND METHODS

### Samples

#### *Spanish amber*

The majority of Mesozoic ambers from Spain are Albian in age (ca. 105My, Cretaceous). Most of the more than 120 Cretaceous amber localities known in Spain are distributed in a curved strip from the east to the north of the Iberian Peninsula which corresponds to the marine coastal line during the Early Cretaceous (Peñalver and Delclòs, 2010). From west to east, amber mainly occurs in the Central Asturian Depression (Ullaga Formation (Fm.), La Manjora Fm. and El Caleyú Fm.), the Basque-Cantabrian Basin (Las Peñas Fm., Bielba Fm. and Utrillas Group; see Barrón *et al.*, 2015) and the Maestrat Basin (Escucha Fm.).

Spanish amber originated from gymnospermous resin produced in resiniferous forests. The palynological assemblages of the amber-bearing outcrops suggest that these forests were subtropical, under a seasonal wet-dry climate, dominated by conifers and inhabited by ferns, other gymnosperms and early angiosperms (Diéguez *et al.*, 2010). Most of the resin remained buried in the forest litter and soil for some time before being transported to definitive deposits in deltaic environments, from freshwater swamps in the Maestrat Basin to marine-influenced deposits in the Basque-Cantabrian Basin and Central Asturian Depression (Peñalver and Delclòs, 2010). These amber deposits contain abundant coal, fusinite, plant cuticles and palynomorphs. The plant cuticles are dominated by cheirolepidiaceans and ginkgoales that exhibit halophyte and xerophilous features; these plants most probably grew in coastal salt marsh environments where the resin pieces were buried (Peñalver and Delclòs, 2010).

Several amber pieces or fragments from diverse Spanish Cretaceous outcrops were screened in order to obtain samples from their cortices. The presence of amber pieces showing cortices is common in all Spanish outcrops and does not depend on the abundance of amber or if the amber contains bioinclusions. However, all the samples studied came from amber outcrops that yielded arthropod

bioinclusions, with the exception of one (Cuchía locality). The outcrops rich in amber pieces having cortices which have been studied are El Caleyú (Oviedo, Asturias; Ullaga Fm.), Cuchía (Cuchía, Santander; Bielva Fm.), Salinillas de Buradón (Álava; Utrillas Group), Peñacerrada I and II (Moraza in Burgos and Peñacerrada in Álava, both from the Utrillas Group), San Just (Utrillas, Teruel; Escucha Fm.) and Arroyo de la Pascueta (Rubielos de Mora, Teruel; Escucha Fm.) (see, Peñalver and Delclòs, 2010).

Small, stalactite-shaped flows and, more commonly, large, kidney-shaped pieces of amber with cortices were studied. Prepared samples from the Salinillas de Buradón and Peñacerrada I and II outcrops are housed at the Museo de Ciencias Naturales de Álava (Álava) (MCNA #) and samples from the San Just and Arroyo de la Pascueta outcrops at the Fundación Conjunto Paleontológico de Teruel-Dinópolis (Teruel) (MAP-#); the remainder are housed at the Museo Geominero of the Instituto Geológico y Minero de España (MGM#) and Universitat de Barcelona.

The amber pieces were collected during several paleontological excavations using diverse methodologies (see Peñalver and Delclòs, 2010). Most were collected from tons of sediment transported in trucks to washing areas, where cement mixers and sieves were used in order to obtain the complete range of amber sizes, as described in Corral *et al.* (1999) and Alonso *et al.* (2000). Amber pieces were first washed in distilled water; their parts covered by lithified sediment were manually cleaned with a scalpel. Subsequently, an ultrasonic cleaner was used where necessary.

The amber pieces usually presented light brown cortices, and it was only necessary to remove a small flake to determine the presence of networks of filamentous structures using a stereo microscope. The presence of cortices and their expansion inside the amber was easily observed in the fragmented or incomplete amber pieces obtained, thus, a simple polish of the fracture surface was sufficient to discern the presence of these networks, most visible in the limits of the cortex and the non-invaded amber core.

We use the following terminology: bioinclusions (the organisms or organismal remains trapped in resin emissions and which are currently preserved in amber) and bioinclusions-like (the organisms or organismal remains preserved in amber due to past biological invasion/colonization of resin masses).

#### **New Zealand copal**

Some taphonomic observations conducted on Pleistocene kauri pine root systems and copal pieces associated with

them are also discussed in this research. These observations were conducted at a private propriety in Waipapakauri, close to State Highway 1, North Island of New Zealand, by E.P. and X.D., during the 2011 campaign. The copal pieces are housed at the Museo Geominero of the Instituto Geológico y Minero de España and Universitat de Barcelona.

#### **Microscopic analyses**

##### **Stereomicroscopy**

Amber cortices were observed using a Leica S8 APO stereo microscope equipped with a Leica EC3. Images were taken at different magnifications using LAS EZ software.

##### **Light microscopy**

In order to determine the morphological and spatial relationships between the filaments, slides for light microscopy observations were prepared, which included the external, middle and internal zones of the cortices. Selected amber fragments were embedded in an epoxy resin (Epotek 301), in order to preserve the integrity of the samples during the slide preparation. This treatment eliminates the “mirror-effect” of internal cracks when illuminated, according to Schlee and Dietrich (1970); and has been previously used with Cretaceous ambers (*e.g.*, Corral *et al.*, 1999); it also guarantees the conservation of amber, prone to natural oxidation and eventual darkening. The slides are housed at the Museo de Ciencias Naturales de Álava and the Fundación Conjunto Paleontológico de Teruel-Dinópolis.

The samples were observed using a Zeiss Axio Imager D1 bright field/fluorescence microscope equipped with EC Plan-Neofluar 20x/0.50, Plan-Apochromat x40/0.90 oil/glyc/water-immersion and Plan-Apochromat 63x/1.40 oil-immersion objectives. Incident and transmitted light were used simultaneously to resolve some structures. A CCD AxioCam HRc Rev 2 Zeiss camera and Carl Zeiss Axiovision 4.7 Software (Carl Zeiss, Oberkochen, Germany) were used to capture and record the images. An Olympus BX51 microscope was used to study some of the samples, which were photographed using a ColorView IIIu digital camera attached to the microscope.

##### **Scanning electron microscopy in secondary electron mode**

SEM in Secondary Electron mode (SE) is appropriate for the study of the external morphology of microbiota in amber because secondary electron signals give contrast based on topography (Ascaso *et al.*, 2003). Prior to SEM-SE examination, amber samples were fractured in order to expose a clean, fresh surface, and they then were coated with gold. The samples were observed using a DSM 960 A

Zeiss at the Centro de Ciencias Medioambientales-Consejo Superior de Investigaciones Científicas (CCMA-CSIC) in Madrid. In the case of El Caleyú amber the images were taken using a HITACHI model S-4100 at the Servei Central de Suport a la Investigació Experimental (SCSIE) of the Universitat de València.

#### **Scanning electron microscopy in backscattered electrons mode and energy dispersive X-ray spectroscopy microanalysis**

Cortex samples were processed for SEM in backscattered electrons mode (BSE) and observed according to the method established by Ascaso *et al.* (2003) for amber material. The use of SEM-BSE yields high magnification images with contrast attributable to differences in the average atomic number of the target (Joy, 1991). These techniques yield images with exceptionally high magnification and resolution as well as important chemical and topographic information about fossil microorganisms and their embedding amber matrix (Ascaso *et al.*, 2005; Speranza *et al.*, 2010).

For SEM-BSE observation and/or energy dispersive X-ray spectroscopy microanalysis (EDS), the amber fragments were embedded in epoxy resin; after polymerization, the blocks were cut and finely polished (Ascaso *et al.*, 2003). Transverse sections of polished surfaces were carbon coated and examined using a DSM 960 A Zeiss electron microscope equipped with a four-diode, semiconductor BSE detector and a Link ISIS microanalytical EDS system at the CCMA-CSIC, under the microscope operation conditions described in Ascaso *et al.* (2003).

#### **Confocal laser scanning microscopy**

The confocal laser scanning microscopy (CLSM) has been used to study microinclusions in amber, enabling the determination of their three-dimensional (3D) morphology and the direct analysis of their chemical compositions (Ascaso *et al.*, 2003, 2005; Dörfelt *et al.*, 2003; Speranza *et al.*, 2010). CLSM has also been used to study the Precambrian biology (Schopf *et al.*, 2010; Schopf and Kudryavtsev, 2011), yielding important information about preservational history and other taphonomic aspects of permineralized organic-walled fossils.

The study of the autofluorescence (AF) of cortex samples was carried out using a Leica SP II confocal microscope at the Centro de Apoyo a la Investigación (CAI) of the Universidad Complutense de Madrid. The CLSM, with a DMIRE2 inverted microscope with transmitted light and epifluorescence mode, was equipped with specific blue (Ex/Em filters BP 450–490/LP 515), green N2.1 (Ex/Em filters BP 515–560/LP 590) and UV (Ex/Em filters BP

340–380/LP 425) filters. Violet/Blue (405nm), Ar (488nm) and HeNe (543nm) laser diodes were used to generate an excitation beam, and then the resultant emission was filtered using the above mentioned specific filters. The AF emission spectrum (or primary fluorescence) of the amber cortices was determined using a lambda-scan ( $\lambda$  scan) tool. The maximum AF emission was calculated by analyzing regions of interest (ROI) of the CLSM images. To obtain a 3D reconstruction of the cortex samples, stacks of 40–70 single confocal optical sections at 0.5–1  $\mu$ m intervals were obtained and subsequently stored and compiled. CLSM reflection mode was used simultaneously in order to detect mineralized parts in the filamentous structures (Speranza *et al.*, 2010). CLSM image analyses, graphical calculations and 3D reconstructions were carried out using the Leica Application Suite AFL.

#### **Fungal polysaccharide detection using CFW and WGA-FITC**

Samples were not decontaminated to eliminate potential alien compounds in the lumina of the filamentous structure because we conducted direct polysaccharide detection in the walls that constitute this structure. For that reason, decontamination as that one described by Girard *et al.* (2009a) is not suitable for our case. On the other hand, the decontamination described by Girard *et al.* (2008) eliminates recent fungi and other contaminant microorganisms present on the amber surface and in cracks, not microorganismal remains embedded within the amber.

Some extant microorganisms and microdebris show autofluorescence due to cellulose and other natural fluorochromes (Ascaso *et al.*, 2003, 2005; Speranza *et al.*, 2010). In extant fungi, autofluorescence is attributed mainly to cell wall compounds and low-molar-mass fluorescent aromatic compounds (Žizka and Gabriel, 2008). Some differences in hyphal autofluorescence have been assigned to chitin modifications, for example due to its type of integration in the cell wall or response to stress factors (Arcangeli *et al.*, 2000). The potential presence of fungal cell wall compounds in the filamentous structures in the amber cortices was analyzed using CalcoFluor White M2R8 (CFW, Molecular Probes) and Wheat Germ Agglutinin conjugated with Fluorescein Isothiocyanate (WGA-FITC, Sigma Aldrich). Both specific fluorescence stains are extensively used in mycological research (*e.g.*, Bartnicki-Garcia *et al.*, 1994; Hoch *et al.*, 2005; Gonçalves *et al.*, 2006).

The fluorescence brightener of CFW, a stilbene derivative, is a simple and sensitive dye that binds to  $\beta$ -1,3 and  $\beta$ -1,4 polysaccharides (Maeda and Ishida, 1967; Herth and Schnepf, 1980). The CFW stain has become increasingly used as a tool to detect fungal cell wall material because it non-specifically binds  $\beta$ -1,4

polysaccharides, *e.g.*, cellulose or chitin, and  $\beta$ -1,3-glucan (*e.g.*, Maeda and Ishida, 1967; Gonçalves *et al.*, 2006). WGA is a sugar-binding protein (lectin) from *Triticum vulgare*-FITC conjugated with a known affinity for *N*-acetyl- $\beta$ -D-glucosaminyl residues and *N*-acetyl- $\beta$ -D-glucosamine oligomers (*e.g.*, Allen *et al.*, 1973; Meyberg, 1988; Schübler *et al.*, 1996). Because WGA-FITC shows a high affinity for chitin, this dye is used to discriminate fungi in samples from different sources (soils, sediments and biofilms in water) (*e.g.*, Wohl and McArthur, 2001; Gonçalves *et al.*, 2006), and also to discriminate between fungal hyphae and filamentous prokaryotes in soil and fresh water (Wohl and McArthur, 2001). Recently, Ivarsson *et al.* (2011, 2012) used WGA-FITC to detect fossilized fungi in subseafloor basalts and in a volcanoclastic apron.

Under sterile conditions, selected cortex samples were broken to expose the networks of filamentous structures, and subsequently, thin sections were made for staining with CFW. In order to prevent artifacts, which could interfere with stain specificity, chemical or mechanical treatments were not applied to the amber surface during slide preparation. Before staining, the slide-mounted amber sections were analyzed using the  $\lambda$  scan tool to confirm that autofluorescence would not interfere with the detection of specific fluorescence signals produced by the CFW. After that, the slides were washed three times with sterile distilled water (for 10min each wash) and then stained with CFW at a concentration of 100 $\mu$ M in water (Gonçalves *et al.*, 2006). The slide sections were incubated in the dark at room temperature for 2 hours and washed with sterile distilled water to remove excess dye. In our study, in order to improve the detection of the CFW fluorescence signals, the samples were observed using a Confocal Leica TCS SP5 equipped with a multiphoton detector at the Servei de Microscòpia- Universitat Autònoma de Barcelona. The conditions established for CFW excitation and detection of emission signals were those described by Hickey *et al.* (2004).

For staining with WGA-FITC, cortices were broken under sterile conditions, and the internal zones with abundant filamentous structures were embedded in Spurr resin. After polymerization, the block was cut using an ultramicrotome and semi-thin sections of 5 $\mu$ m were obtained and mounted onto glass slides that had previously been coated with poly-Lysine (5mg/mL) (Sigma) at the Instituto de Ciencias Agrarias-CSIC (ICA-CSIC) in Madrid. In order to eliminate the AF background of the amber cortices, which can overlap with the WGA-FITC emission spectrum, the semi-thin sections were irradiated with UV light (30W, 253nm to 400nm discrete emission) (photobleaching) at room temperature (Viegas *et al.*, 2007). The samples were monitored every 5 minutes with a Zeiss Axio Imager D1 microscope in the epifluorescence mode to detect reduction in the AF background. Successful

photobleaching of the cortex samples, in order to eliminate the AF background, was confirmed using the CLSM  $\lambda$  scan tool. In consequence, WGA-FITC fluorescence signal from the filamentous structures stained was detected although amber is a fluorescent material. CLSM observations were carried out using a Leica SP2 Confocal microscope from the Servicio de Técnicas No Destructivas (STND) of the Museo Nacional de Ciencias Naturales-CSIC in Madrid.

Next, the slides containing the cortex semi-thin sections without AF background, were incubated with WGA-FITC at a concentration of 50 $\mu$ g/mL in 10mmol/L phosphate buffer for 2 hours, as described by Meyberg (1988). After incubation, the samples were washed three times (for 10min each wash) with sterile distilled water to remove excess dye, a cover slip was applied and the samples were examined immediately. The conditions established for WGA-FITC excitation and detection of emission signals were those described by Schübler *et al.* (1996). However, a longer period of laser excitation was required to recover WGA-FITC emission signals, and special care had to be taken in order to avoid laser damage to the semi-thin cortex samples. Stacks of 5–21 single confocal optical section images were prepared at 0.2–0.5 $\mu$ m intervals for all the samples stained with WGA-FITC. CLSM image analyses, graphical calculations and 3D reconstructions were carried out using the Leica Application Suite AFL. The slides are housed at the Museo de Ciencias Naturales de Álava and the Fundación Conjunto Paleontológico de Teruel-Dinópolis.

## RESULTS

The opaque, light brown cortices present in different types of Spanish amber pieces had a similar appearance (Fig. 1). In general, the width of the cortex was largely regular in each piece (Fig. 1E–F). Only a few of the stalactite-shaped amber pieces showed a cortex, and where present, it was generally thin (Fig. 1E). Most of the kidney-shaped amber pieces showed thick cortices (Fig. 1A–B, F). Some atypical pieces showed cortices that irregularly invaded the amber pieces, forming conspicuous, heterogeneous expansions toward the interior (Fig. 1B, C). Despite the large size of most of the kidney-shaped amber pieces, their cortices sometimes occupied the entire amber mass (Fig. 1G), a phenomenon which was never observed in the stalactite-shaped amber pieces; it has also been reported for some French Cretaceous amber pieces from the Fourtou locality (Girard *et al.*, 2013).

Dense networks of filamentous structures constituted all cortex samples observed (Figs. 2A–D; 3–5; IB–E; II; IIIA–E); Waggoner (1994a) was the first to note this feature in non-Spanish amber. Three cortex zones in amber pieces

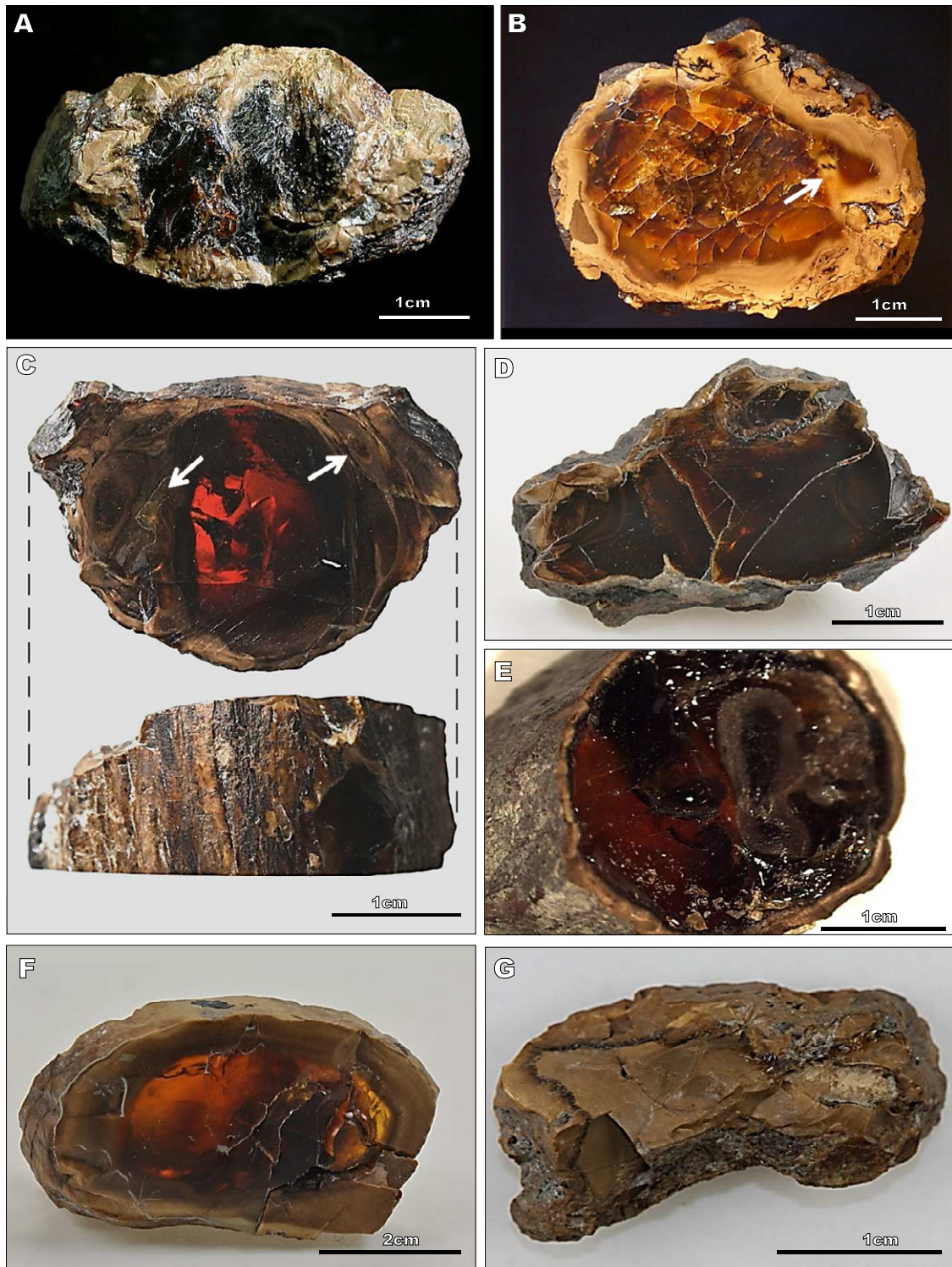


**FIGURE 1.** Diverse aspects of the Spanish amber cortices. The two main types of amber pieces, kidney-shaped pieces (A, B, D, F and G) and stalactite-shaped pieces (C and E) from Salinillas de Buradón (A), Peñacerrada (B), San Just (C–E) and Cuchía (F and G) localities. A) Unpolished and B) polished kidney-shaped pieces, housed at the Museo de Ciencias Naturales de Álava (MCNA), showing irregular expansions of the cortices to the amber core (MCNA 14868 and MCNA 14422, respectively; Photos R. López del Valle). C) Partially polished stalactite-shaped piece, housed at the Fundación Conjunto Paleontológico de Teruel-Dinópolis (MAP-4464), showing several fungal growths in several resin flows. Note the first main flow as a cylindrical core slightly invaded by the fungus. D) Polished kidney-shaped piece showing a cortex of irregular thickness (sample subsequently prepared, see Fig. 2E). E) Stalactite-shaped piece section showing a thin cortex of homogeneous thickness (sample subsequently prepared; see Fig. 2F and details in Fig. 3). F) Polished kidney-shaped piece (MGM10675C) showing a thick cortex of homogeneous thickness. G) A kidney-shaped piece completely invaded by the fungus (MGM10676C). Arrows in B–C indicate conspicuous, heterogeneous expansions of the cortices toward the interior.

preserving a core of transparent amber and a thick cortex have been differentiated: external, middle and internal (Fig. 2C–D), the latter being in contact with the amber core. The filaments were denser at the external zone (periphery) of the cortices, and became sparse toward the amber core (Fig. 2A–D). In a few cases, the cortices show isolated laminae within successive resin flows (Fig. 3A) or bands (Fig. IA, Electronic Appendix available at [www.geologica-acta.com](http://www.geologica-acta.com)).

Filaments were slightly flexuous, with a diameter of about 5–8 µm. Branching was rare, but when present the distance between bifurcated branches was about 20–30 µm and the branching angles ranged between 70° and 90°. Scarce septate filaments were observed. In general, dark brown filaments were located in the external cortex zones (Figs. 2E–F; 3A–C; IA). Most of the cortices were composed of yellow-beige filaments which became translucent and less dense in the internal part of the amber pieces (Figs. 2A–D; 3D–F; IB–E; IIA–E). Light microscopy observations indicated that the filaments were constituted by an empty core (diameter ~1–2 µm) and a halo (thickness ~2–3 µm) (Figs. 3B–F; II). However, there were some differences in the filaments depending on their location: in the internal zone of the cortices, the filaments showed buds and knob-like protuberances arising from their internal parts (Figs. IID–E; IIID). Spores and structures that could definitely be interpreted as reproductive structures of fungal origin were not observed. In all amber cortices observed by light microscopy, the basic form and size described remained more or less homogeneous (Figs. 3; I; II).

SEM (BSE and SE) and CLSM observations (Figs. 4–5; IIIA–E) supported the structure of the filaments observed in the studied samples. In general, the filaments that were translucent under LM, the most abundant typology, showed both an empty core and a surrounding halo under SEM (Figs. IIIA–B). However, the filaments from the external cortical zone that were opaque under LM (Figs. 3B upper part; IA) were bright under SEM-BSE (Fig. IIIC–E). This brightness indicated the presence in the filaments of compounds with a higher atomic number: S and Fe, as determined by EDS analyses (Fig. IIIF). The mineralized filaments became less abundant in the internal cortical zone (Fig. IIIC). Although some constriction and/or fragmentation could be observed in the internal parts of the mineralized filaments, no septum or septum-like structure could be identified with confidence (Fig. IIID).

Under SEM, an inconspicuous limit is present between the halo and the surrounding amber in almost all samples (Fig. IIIA–B). In other samples, holes are evident in the external surface of the halo (Fig. 6B–C), which may be crossed by abundant empty radial fibrillar structures. This appearance is associated with the loss of amber located at the end of the empty radial fibrillar structures, which can be

very advanced implicating the isolation of the filamentous structure from the amber. Marcasite/pyrite precipitates may be present.

The relatively good translucence of the amber enabled us to perform a 3D reconstruction of the filamentous structures. The external zones of the cortices were observed by CLSM, revealing a high autofluorescence that corresponded to the non-mineralized filaments (green false color in Fig. 4A, C), while the mineralized filaments only reflected the laser signal (blue false color in Fig. 4B, E). The maximum fluorescence emission by the filamentous structures determined using the CLSM  $\lambda$  scan tool and calculated based on the analyses of several ROI was detected between 550 and 570 nm.

Autofluorescence became more evident in filaments from the middle and internal zones of the cortices, and in combination with the 3D reconstruction a sharp image was obtained (Fig. 4A, C). When the two types of signals detected by CLSM were integrated, it was possible to see that mineralization was more intense in the filaments from the external cortex zones (Fig. 4C), confirming the SEM-BSE observations (Fig. IIIE). Filaments with both mineralized and non-mineralized parts were frequently observed, indicating that the mineralization process was not homogeneous.

Amber cortex slides stained with CFW revealed the presence of cellulose or chitin, and  $\beta$ -1,3-glucan (Fig. 4F). Filaments from all the samples analyzed showed a CFW-positive stain which produced the fluorescence that was observed by CLSM (red false color in Fig. 4F). Filaments showing mineralized parts were frequently observed (blue false color in Fig. 4E), but the most abundant were the filaments showing CFW fluorescence signals (red false color in Fig. 4F). Using CFW, polysaccharides were located in all filaments, but specific areas of occurrence were not discriminated (Fig. 4F).

In cortex sections treated with UV light for photobleaching, the elimination of the AF background reached its peak after 15 minutes of treatment. Because the use of CFW did not allow unequivocal detection of chitin, it was investigated the WGA-FITC staining patterns in more detail (Fig. 5). The WGA-FITC fluorescence signals, produced by the binding of this biomarker to chitin, specifically to *N*-acetylglucosamine oligomers from chitin, showed a specific and constant distribution in the filaments. The filaments showed unequivocal WGA-FITC fluorescence signals (yellow false color in Fig. 5) in some areas with a dotted appearance. Only the filaments were reactive to the two biomarkers, and no specific fluorescence signals were observed in the amber matrix, thus it was detected specific fluorescence signal as evidence for the presence of chitin (Fig. 5).

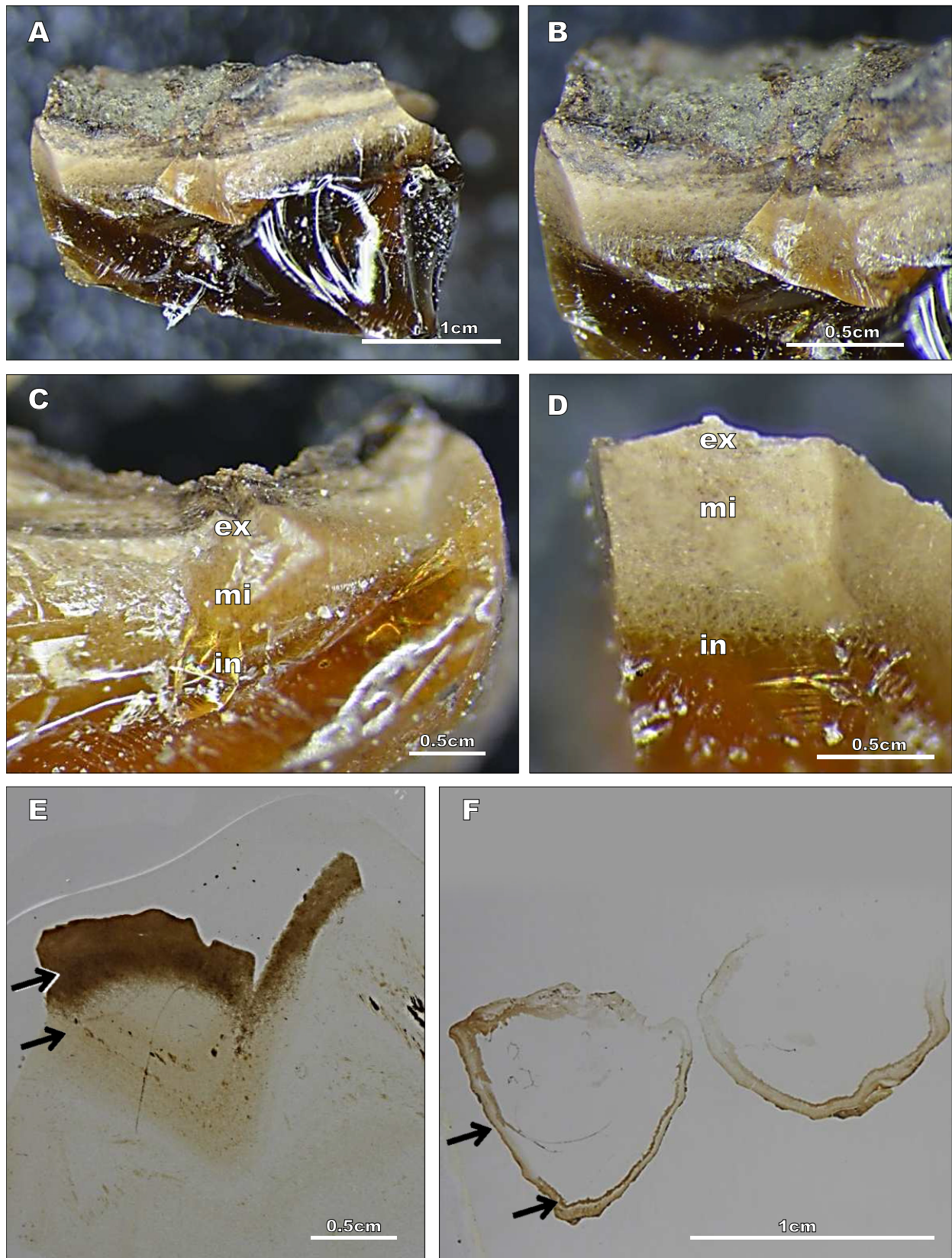


**FIGURE 2.** Detail of the Spanish amber cortices from San Just (A and B) and Cuchía (C and D), showing the external (ex), middle (mi) and internal (in) zones of the cortices composed of profuse fungal mycelium. E) and F) Thin sections from a San Just kidney-shaped piece (E; fragment: MAP-4470) and a San Just stalactite-shaped piece (F; two complete sections: MAP-4471) showing fungal colonization (arrows).

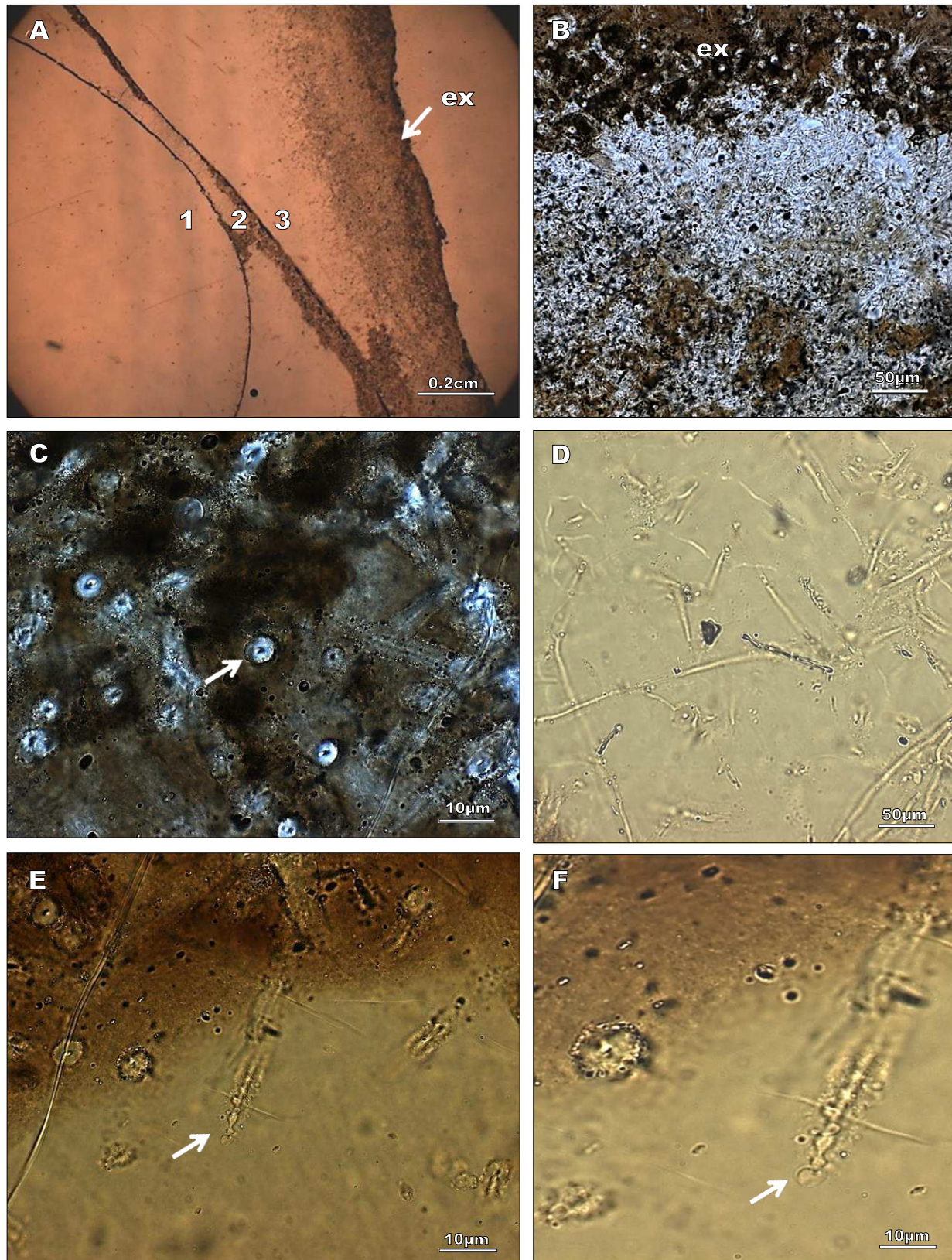


**FIGURE 3.** Light microscopy images of a stalactite-shaped amber piece from San Just outcrop (MAP-4471; see Figs. 1E and 2F). A) Note that each successive resin flow (1–3) shows a fungal colonization, being the mycelium more profuse in the last flow (3). B) and C) The mycelium from the external zone (ex) is strongly mineralized, showing mineralized lumen hyphae (e.g., arrow in C). D–F) Hyphae became sparse and hyaline toward the internal zone (arrows).

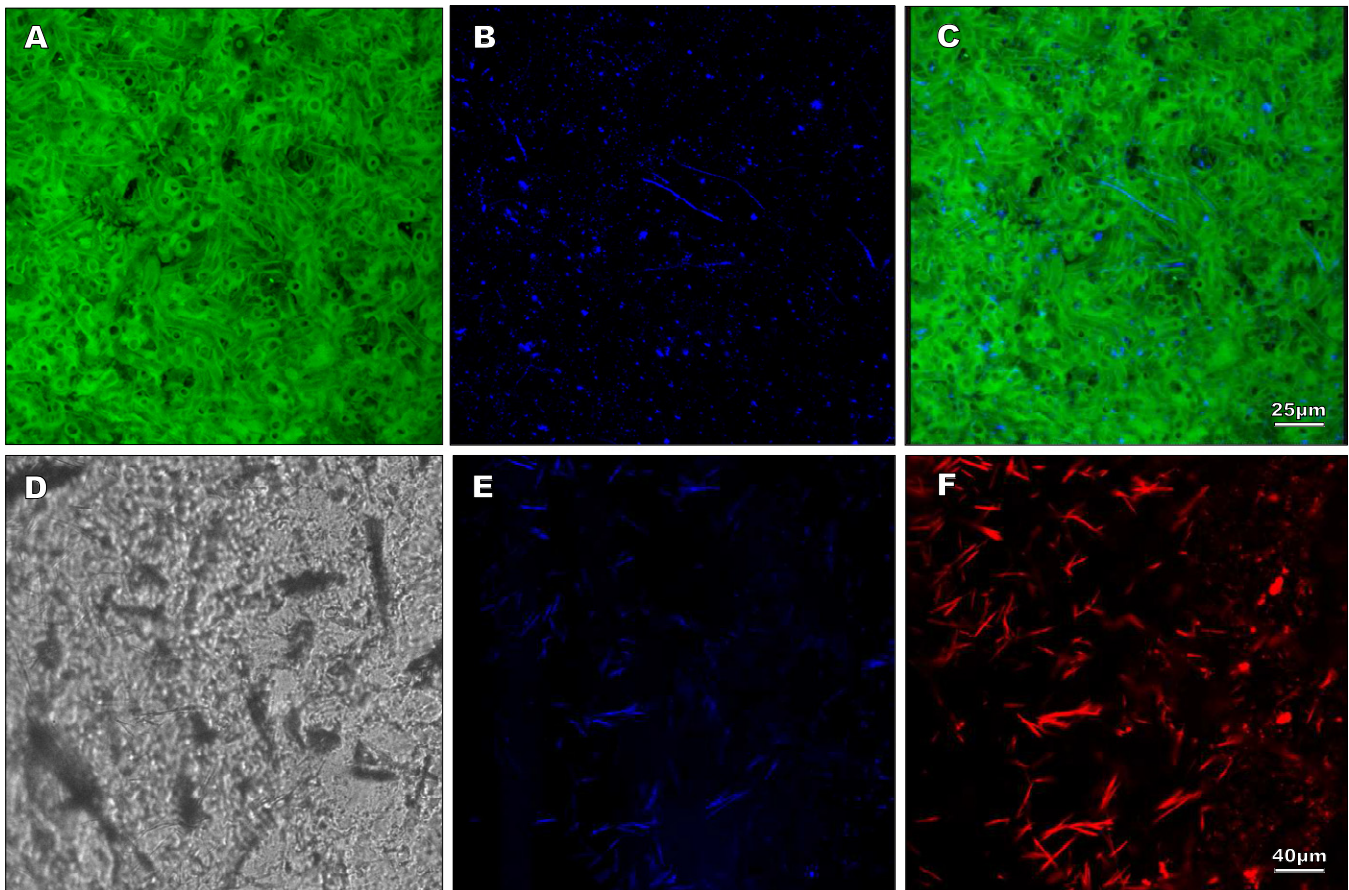


**FIGURE 4.** CLSM images of filamentous structures in cortices from Salinillas (A–C) (sample not conserved) and San Just (D–F) (MAP-4467) ambers. A–C) CLSM images of the same area showing A) non-mineralized hyphae (green) and B) mineralized hyphae (blue); C) is the combination of both hyphae preservations (A and C = 3D-reconstructed series of confocal sections). D) CLSM image of an unpolished slide in the same area observed in (E) and (F) but obtained in reflected laser light. E) CLSM image showing mineralized hyphae (blue). F) Same area after CFW stain showing strong fluorescence signals (red) which reveal the presence of conserved polysaccharides in the hyphae.

## DISCUSSION

Fungi are exquisitely preserved in ambers from diverse sites and geological ages (*e.g.*, Poinar and Singer, 1990; Rikkinen and Poinar, 2000; Ascaso *et al.*, 2005; Peñalver *et al.*, 2007; Speranza *et al.*, 2010). In recent decades, due to the discovery of new highly fossiliferous amber deposits and the significant increase in the number of publications, diverse controversies about the misinterpretations of microorganisms and microscopic structures included in amber have been published (Grimaldi, 2009; Thorn *et al.*, 2009). The study of microorganismal inclusions requires a multidisciplinary approach using diverse techniques; firstly, in order to avoid several potential problems such as the study of artifactual pseudofossils as true fossils, and secondly to improve the interpretation of the morphological evidence used in taxonomic classifications and the use of chemical evidence. This is one of the most troublesome problems confronting paleontologists, paleomicrobiologists and microbiologists, especially if we consider that, for

example, the available information corresponds to the morphology of a single phase of the fungal life cycle or of other microorganisms, or corresponds to published photomicrographs of low quality that do not permit a convincing identification (Thorn *et al.*, 2009; Grimaldi, 2009).

We should not rule out that more than one taxon is present in some parts of the cortices, but the subject of the present study is the fungus that strongly invaded the pieces and originated the mycelia which constitute the cortices. With respect to this microstructure, Poinar (1992) was the first to indicate its morphological similarity to fungi, based on specimens present in German Cretaceous amber (originally considered Triassic in age). Later, Poinar *et al.* (1993) assigned it to sheathed algae (see Fig. 1G in Poinar *et al.*, 1993). In general, previous authors who have studied this filamentous structure in different ambers have reported strong similarities with fungal mycelia, but have assigned it to different microorganismal groups.

Based on morphological characteristics, these filamentous structures have been interpreted as prokaryotes, giving very succinct descriptions but providing scant evidence to support their conclusions (*e.g.*, Poinar, 1992; Poinar *et al.*, 1993; Waggoner, 1994a; Waggoner, 1996; Schmidt and Schäfer, 2005; Breton and Tostain, 2005). Morphological features specific to fungi, such as mycelial networks, hyphal anastomosis, pore and septa ultrastructures, and spores and fruiting bodies, can be used to distinguish them from prokaryotes; however, these structures are commonly absent or, when present, may sometimes be subject to diverse interpretations. Distinguishing between fossilized fungal hyphae and filamentous prokaryotes found as amber inclusions based on morphology alone can be extremely difficult. Biomarkers specific to fungal chitin have recently been used successfully to detect chitin in association with specific fossilized microorganisms in geological materials (Ivarsson *et al.*, 2011, 2012).

The fungal nature of the filamentous structures constituting the Spanish amber cortices is supported by morphological, cytochemical and taphonomic evidence, as are explained in detail below. However, the lack of preservation of diagnostic characters in these fossil fungal mycelia prevents a proper systematic assignment within the major clades of the Kingdom Fungi. Also, based on taphonomic evidence is clear that this structure is Cretaceous in age. Its fungal nature has varied implications that are also discussed below. To better follow the next discussion, after the detection of chitin, the morphological terms will be named subsequently as the fungal parts that represent.

### A fungal origin according to morphology and cytochemistry

Within the eukaryotic domain, fungi form a monophyletic clade that *sensu stricto* comprises a heterogeneous, often inconspicuous group of microorganisms which are primarily heterotrophic with an osmotrophic style of nutrition and contain chitin and  $\beta$ -glucans in their cell wall (Voigt and Kirk, 2011). These characteristics enable them to be distinguished from other microorganisms. Fungi have a filamentous branching system of cells (hyphae) that extend by tip growth, and lateral branching creates a fine network called the mycelium. The hyphae usually consist of a tubular cell containing different organelles within a cytoplasmic membrane that is surrounded by a rigid, chitin-containing cell wall.

The results obtained using LM, SEM, SEM-BSE, CLSM and polysaccharide stains observed by CLSM were considered together. The shape and size of the filamentous structures fit well with fungal hyphae rather than a prokaryotic origin.

Although the fossil mycelium was sparsely branched, it should be borne in mind that fungal morphology can vary depending on the composition of the medium in which the hyphae grew. Only a few hyphal septa were observed; however, it cannot be ruled out that this structure may have been almost completely degraded in the Spanish samples if originally present. The spatial arrangement of the filament in the amber fits well with a typical hyphal network. The buds and knob-like protuberances observed (Figs. 3; II) resembled hyphal modifications present in extant basidiomycetes (Stalpers, 1978) more than bud-like reproductive structures. Previous authors who have studied

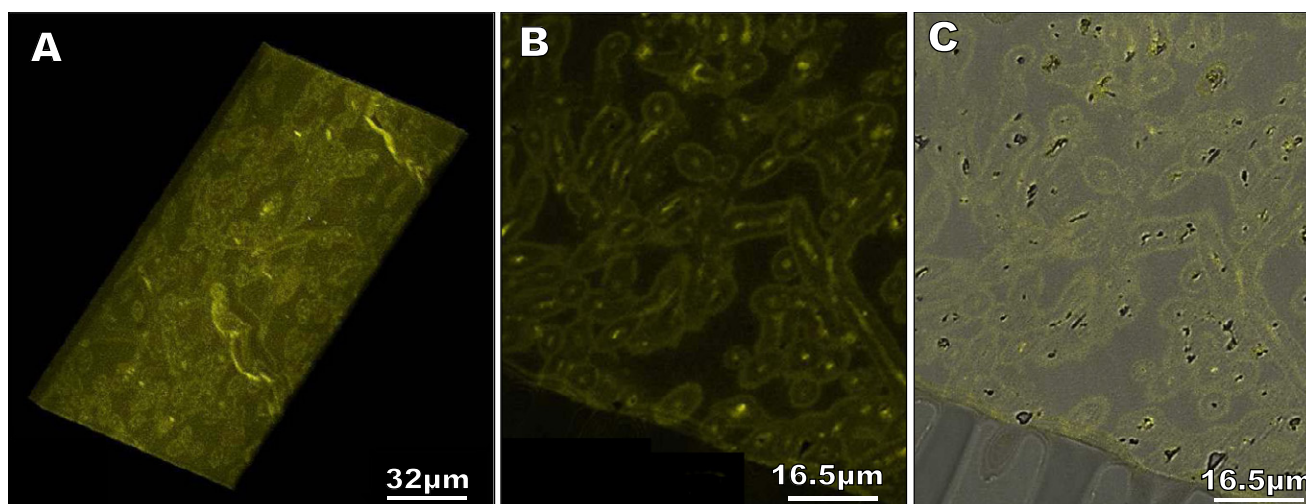


**FIGURE 5.** CLSM images of WGA-FITC stain of filaments from a San Just amber cortex (MAP-4466) showing fluorescence signals (yellow) that correspond to chitin molecules present in the fungal cell wall and lumen. A) 3D-reconstructed series of confocal sections of amber cortices semi-thin sections. B) and C) Detail of the chitin localization in the fossil fungal hyphae (C: combination of transmitted and CLSM images).

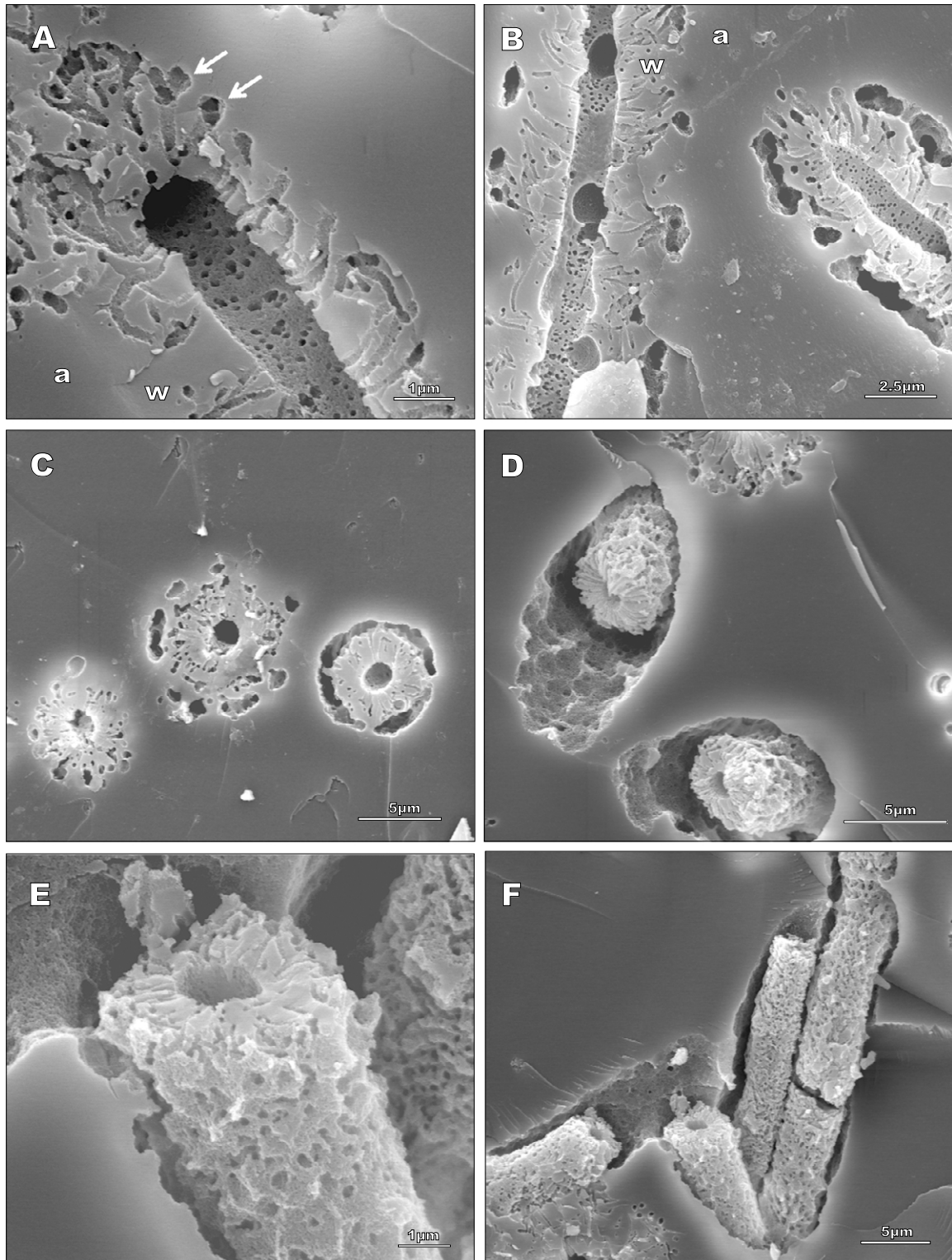


**FIGURE 6.** SEM photomicrographs of hyphae from El Caleyú amber cortex (Upper Albian) showing different stages of hyphae degradation in the same sample obtained making a simple fracture of the cortex. A) Longitudinal section of a hypha in stage 1 (note incipient peripheral holes: arrows) showing cylindrical lumen with abundant holes from which radial empty fibrillar structures that cross the wall arise. Note the apparent continuity of the hyphal wall (w) and the surrounding amber (a). B) Two longitudinal sections of two hyphae in degradation stage 2 showing peripheral holes, mainly the right hypha. C) Three transversal sections showing degradation stage 2 most pronounced from the left to the right of the image (right hypha showing a nearest stage 3). D) Two oblique sections showing hyphae in degradation stage 3 (note the isolation of the wall from the strongly degraded amber). E) Hypha in degradation stage 3 showing the high degradation of the wall. Note the irregularly eroded appearance of the wall. F) Several hyphal fragments practically isolated from the surrounding amber. a: amber, w: hyphal wall.

similar networks of filamentous structures in other ambers have not described septa, but have described putative cells that in our opinion were most probably artifacts originated from mineral infillings of the lumina or expansions of the lumina, possibly due to degradation.

The cell wall is a unique structure common to all fungi and acts as an interface between the fungus and its environment. The cell wall is composed of a semi-permeable fibrillar network of polysaccharides, which confers mechanical strength for maintaining cell shape and integrity, as well as providing protection from various environmental stresses. In extant fungi, three basic components represent the main polysaccharides of the cell wall: glucans, mannans and chitin, which account for 80–90% of the mass of the fungal cell (Lalgé and Calderone, 2006). Glucan and chitin, the main components of the cell wall, are unique to fungi (Lalgé and Calderone, 2006). The main glucan component from the fungal cell wall is  $\beta$ -1,3-glucan, which is composed of long linear chains of  $\beta$ -1,3-linked glucose, whereas chitin is a  $\beta$ -1,4-linked linear homopolymer of *N*-acetylglucosamine.

Glucan and chitin represent the neosynthesis of a cell wall in the Kingdom Fungi; therefore, changes during fungal evolution consisted mainly of modification of the  $\beta$  glucan-chitin skeleton (Bartnicki-Garcia *et al.*, 1994; Lalgé and Calderone, 2006). Chitin is the most ancestral fungal cell wall structural polysaccharide, and although it is considered a relatively minor component of the fungal cell wall, it constitutes an essential compound for maintaining the integrity of this structure. The schematic organization of the cell wall in extant yeasts and filamentous fungi consists of a central core of the cell wall composed of branched  $\beta$ -1,3/1,6 glucan, which is linked to chitin via a  $\beta$ -1,4 linkage (Manners *et al.*, 1973a,b; Fontaine *et al.*, 2000). The central core is present in most fungi and at least in all Ascomycetes and Basidiomycetes, but is differently organized depending on the species. Models of fungal cell wall structure and component location have only been established for a few fungal species (Lipke and Ovalle, 1998; Bowman and Free, 2006). According to these models, most of the chitin is considered to be located near to the cytoplasmic membrane, whereas in other models, the  $\beta$ -1,3-glucan could be located throughout the entire wall (Lipke and Ovalle, 1998; Bowman and Free, 2006).

The internal part of the fossil filaments is interpreted as remains of hyphal cytoplasmic membranes and/or the internal part of fungal cell wall components, which maintain a close spatial relationship in extant fungi. This part presented various degrees of preservation, showing different intensities of fungal polysaccharide signals (Fig. 4F), or was completely mineralized (Fig. 4B). Both  $\beta$ -1,3 and  $\beta$ -1,4-linked fungal polysaccharides were detected in

the filamentous structures in all cell wall layers, including the hyphal surface and inner layers, as shown by clear WGA and CFW labeling (Fig. 5). This pattern of polysaccharide distribution evidenced by specific fluorescence signal fits well with that observed in damaged fungal cell walls; mechanical damage produces an increase in the cell wall pore size, allowing greater labeling of the native wall compounds that are not normally exposed on the surface (Nicole and Benhamou, 1991).

The observed halo in the fossil fungi corresponds to a thick cell wall, as in several other extant fungal species previously reported (Lipke and Ovalle, 1998; Bowman and Free, 2006). The empty radial fibrillar structures clearly visible in Figure 6 and illustrated in Figure 7 are interpreted as the matrix produced by degradation of structural polysaccharides from the fungal cell wall skeleton.

The presence of an external mucilaginous part and/or remains of cell wall incrustation in the original fungi should not be ruled out (Figs. 3C–F; IIC–D). The production of a mucilaginous polysaccharide sheath around extant fungal hyphae is a widespread strategy employed by several fungi to interact with different substrate types (wood, stones, mineral clays, plant roots) when growing inside them (Vesentini *et al.*, 2005). This mucilaginous sheath is involved in several fungal functions, such as substrate degradation, protection and stress resistance (Burford *et al.*, 2003; Vesentini *et al.*, 2007). Although bacteria have mucilaginous sheaths, given both the cell wall organization and its chemical composition, the present results clearly rule out the possibility of a bacterial nature (Hoiczky and Hansel, 2000; Pereira *et al.*, 2009).

The chemical composition of the mineralized hyphal structures observed by SEM-BSE, which consisted mostly of S and Fe (Fig. IIIF), fits well with the composition of fossilized fungal hyphae previously found in amber, in subseafloor basalts and in turtle eggs from the Lower Cretaceous (*e.g.*, Ascaso *et al.*, 2003; Speranza *et al.*, 2010; Ivarsson *et al.*, 2011).

The chitin and polysaccharide signals detected in the filamentous structures in Spanish amber are of great interest due to the age of the amber (Albian, ca. 105My), the high degree of preservation that has enabled detection of these specific fluorescence signals and the clear evidence indicating that the fossil microorganism is a fungus. Generally, polysaccharides and structural proteins are considered unpreserved in ancient fossils because they are readily degradable through microbial chitinolysis and proteolysis. Chitin is a labile molecule; however, when complexed with proteins it may be resistant to decay under certain conditions (Flannery *et al.*, 2001). Briggs (1999) discussed the main factors involved in chitin preservation

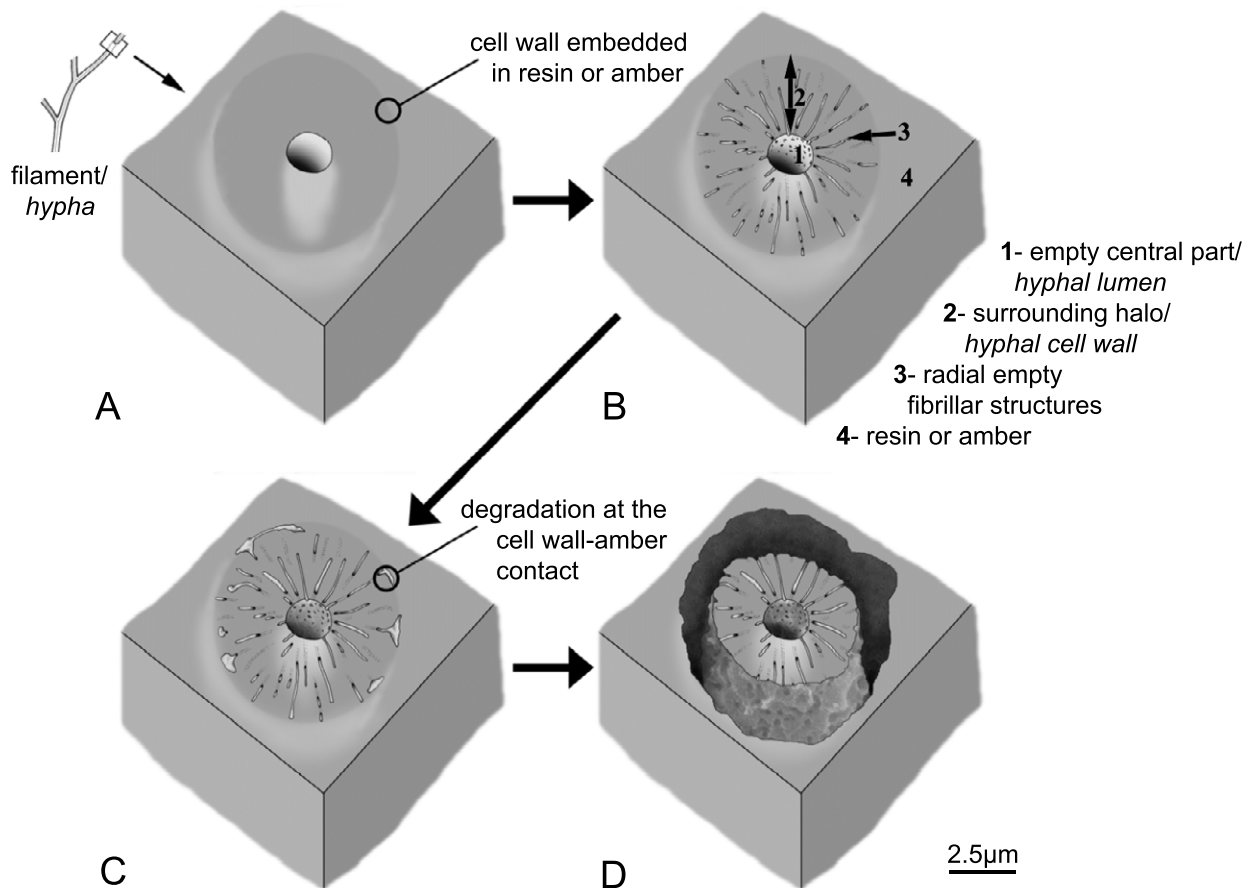


**FIGURE 7.** Cross-section of a fungal hypha and sequence of its degradation based on an amber cortex sample from El Caleyú amber (Upper Albian), according to the model proposed in the present article. A) and B): Stage 1. C) Stage 2. D) Stage 3. See section Taphonomy in the main text for details.

over a long time scale, and he also indicated that such preservation without a complete diagenetic alteration is very uncommon even in amber, which encapsulates the fossil, eliminating almost all external factors.

### Taphonomy

#### Biostratinomy

Breton and Tostain (2005) interpreted similar filamentous structures as a cyanobacterial felting (= cyanobacterial mat) trapped in resin; thus, they considered it a typical bioinclusion. However, they noted a taphonomic incongruence according to their interpretation, which is that the resin flows did not guide the filamentous structures, whereas the impurities of the original resin were oriented. Evidently, a flow of resin covering a delicate mat would have strongly altered the structure. Thus, given the spatial organization of the filamentous structures, these fossils are not true bioinclusions, in contrast to Breton and Tostain's interpretation. Schmidt and Schäfer (2005) interpreted this taphonomic evidence correctly, indicating

that the filamentous structures had invaded the resin and grown inside it, as has been documented in extant sheathed bacteria (Schmidt and Schäfer, 2005.); Girard *et al.* (2009a) indicated the possibility that both mechanisms occurred, depending on the samples. However, these latter authors did not provide any evidence suggesting potential amber preservation of the polysaccharide-protein-lipid complexes that constitute the sheaths of sheathed bacteria and the gelatinous wall of cyanobacteria (Hoiczyk and Hansel, 2000; Pereira *et al.*, 2009). This fact fits well with fungi growing inside resin (bioinclusions-like) instead of occasional resin trapping of cyanobacterial mats (bioinclusions). Future cytochemical evidence may help discriminate with confidence between a bacterial or fungal origin for the cases of French and German cortices.

The different origin in the trees of the two main types of resin/amber pieces also supports a fungal nature. The trapping of cyanobacterial mats by stalactite-shaped pieces which originated under aerial conditions on branches and trunks is implausible. Based on our *in situ* observations (X.D. and E.P.) of Pleistocene kauri root systems in North

Island of New Zealand in 2011, the kidney-shaped pieces are interpreted as largely originated in the roots within the soil, thus in burial (confined) conditions (Fig. 8), and occasionally within the litter (Fig. 8). In these Pleistocene root systems we found abundant kidney-shaped pieces of copal attached to the roots and covered by original soil. Henwood (1993) indicated that in tropical-subtropical forests, resin could solidify on or within the soil. In addition, several features of the amber pieces, mainly the lack of flow input features separated by desiccation surfaces, unlike stalactite-shaped pieces, suggest that they originated within the soil.

Further taphonomic evidence on Spanish ambers is not consistent with the interpretation of Breton and Tostain (2005), followed by Girard *et al.* (2009a) in some cases. It is that the filamentous structures of biogenic, microorganismal origin were generally present on the entire external surface of the amber piece, not only in some parts, as would be expected in the case of a typical embedding in resin flows. This was especially clear in the kidney-shaped pieces, and a plausible explanation would be that the microorganism was a fungus present in the litter and soil that rapidly colonized the entire external surface of the resin pieces, perhaps also inducing the root to exude resin. Filamentous fungi are considered more adapted to growth on non-liquid substrates than yeasts or bacteria, because the hyphal network offers additional avenues for new nutrient exploration (Wu *et al.*, 2008). Colonizing microorganisms must have certain metabolic and physiological characteristics, such as the capacity to synthesize phenoloxidase and resinase enzymes, in order to use resin compounds as a carbon source for growth on this special substrate (Martínez *et al.*, 2005).

The abundance of Spanish amber pieces, ranging from small to large in size, which are completely invaded by the filamentous structures (Fig. 1), constitutes the definitive evidence against an embedding process of mats. Breton (2007) provided a detailed discussion of his interpretation of the origin of these fossils as typical embedding of mats in resin flows or true bioinclusions, citing as evidence (in his figure 1) an amber piece with typical peripheral areas or cortex, but with irregular expansions to the interior and isolated areas within the unaltered internal amber. According to his figure, the areas were not originally isolated, because the amber piece is not complete (it is broken and lacks some peripheral portions) and shows some inner parts apparently isolated from the lost periphery. Irregular growths in some Spanish amber pieces (Fig. 1B, C) have been observed, and in their figure 5, Girard *et al.* (2009a) presented a similar piece as proof indicating that the cortices did not originate from modern amber degradation, because modern growth can not originate in an inside part of the amber pieces which is isolated from the external environment. These records

can easily be explained by different times of solidification of some parts of the resin pieces. Due to the accumulation of resin, through internal inputs that increase the size of the piece by distension in kidney-shaped pieces (Fig. 1A–D, F) and by accumulative flows in stalactite-shaped pieces (Figs. 1E; 3A), solidification of the pieces could be inhomogeneous, implying fungal growth depending on the diverse resin zones.

The abundance of this fungus suggests that the resin itself was its primary substrate. In view of the above explanation, the Spanish cortices at least clearly originated through one of the three primary taphonomic mechanisms for the incorporation of fungi into amber listed by Hower *et al.* (2010): the resinicolous fungi using the resin as a carbon source. Various extant resinicolous fungal species have been described included in amber (Rikkinen and Poinar, 2000, 2001). Most resinicolous fungi seem to be opportunistic saprobes or possibly weak parasites (Hawksworth and Sherwood, 1981; Boddy *et al.*, 2008). They have the ability to grow under conditions of low oxygen concentration, low water availability and presence of toxic resin compounds (Hintikka, 1970; Rikkinen and Poinar, 2000).

The study of the large kidney-shaped copal pieces at the Pleistocene kauri deposits, which were formed by root exudates of resin into the soil, reveals that this type of piece remained soft (non-solidified resin) for a long time due to the conditions of confinement, which involved the maintenance of moisture. This could explain the presence of the thick cortices in several pieces and the occurrence of resin masses completely colonized by the fungus, due to the long time available for fungal growth before curing of the resin (Fig. 1G). In contrast, only a few stalactite-shaped amber pieces (mainly small to medium in size) showed cortices (Fig. 1E). These pieces were only slightly colonized because when they fell to the ground they were already largely solidified. According to these scenarios, aquatic conditions were not necessary; thus, growth could occur under the normal, usually wet soil and litter conditions of subtropical forests.

Some of the stalactite-shaped pieces (Fig. 1E) from Spanish outcrops showed growths between different resin flows (Figs. 3A; IA), as was also observed by Schmidt and Schäfer (2005) in German amber pieces. This observation could only be explained if fungal spore or mycelium colonization occurred in fresh resin emissions under aerial conditions. The colonization may have taken place several times due to subsequent episodes of resin emission. Under aerial conditions, fungal growth would have been short due to rapid solidification of the resin. In Spanish pieces, it is clear that the fungal growth was directed to the fresh resin of a new flow from the external surface. Stalactite-

shaped pieces from El Soplao and San Just showing incipient growths suggest a notably rapid solidification of resin emission. These observations are additional evidence which discard the hypothesis that cortices are caused by Recent fungi that grow within amber.

Knight *et al.* (2010) reported a different fungal mycelia morphotype in Upper Cretaceous (Santonian) amber from eastern Alabama (USA), which occurred in layers without associated plant debris. These authors concluded that fungi grew on the surfaces of fresh resin and were then entombed by subsequent resin flows.

#### **Age of the mycelia and cortices**

The previous biostratigraphic data certainly indicate that the fungal mycelia originated during the Cretaceous. Additional observations support that inference.

As in non-degraded Spanish samples, Schmidt and Schäfer (2005) observed in German samples that, under SEM, there is an inconspicuous limit between the filament walls and the surrounding amber, and correctly deduced that the impregnation had occurred before curing of the resin. This evidenced that the filamentous structures originated in fresh resin during the Cretaceous, before curing of the resin and subsequent fossilization process. Dal Corso *et al.* (2013) demonstrated that the growth of this microorganism in San Just amber pieces did not change carbon-isotope composition values ( $\delta^{13}\text{C}_{\text{amber}}$ ) in the amber, thus it used resin/amber compounds as a resource to grow inside the pieces. Several of the amber pieces studied, obtained *in situ* from the San Just stratigraphic levels, were original fragments from resin pieces with cortices, not complete pieces with cortices. Because these pieces were obtained from the stratigraphic levels without fragmentation or loss of material, it is clear that the fragmentation of the original pieces occurred during the Cretaceous, most likely due to water transport kinetics. These original fragments are composed of a portion of unaltered amber core with a portion of cortex; both portions in the same fragmented piece showed polished surfaces due to water transport. This could only have originated when large resin pieces with a cortex broke during the Cretaceous and the fragments were polished during transport before final burial and fossil diagenesis. This evidenced that the filamentous structures are Cretaceous in age; it is in accordance with the conclusions by Schmidt and Schäfer (2005) and Girard *et al.* (2008) based on different evidence.

#### **Fossil diagenesis: amber and hyphae degradation**

Cortices constitute a very important taphonomic factor that sometimes completely or partially altered the typically exceptional preservation of the arthropod

bioinclusions. As has been indicated by Dal Corso *et al.* (2013), the features and location of the filamentous structures from the external surface to the interior of the amber pieces favored the degradation of the amber during fossil diagenesis and also during weathering, when amber-bearing deposits are eroded. Amber containing networks of filamentous structures is more fragile. Some of the samples studied revealed that the filamentous structures could show variations in their features, as Waggoner (1994a) observed in other Cretaceous ambers concluding that two taxa were involved in their origin. Under SEM, have been observed that differences in some features were caused by degradation; thus, this fact indicates that only one taxon was involved, at least in the origin of the Spanish amber cortices. The cortex volume is connected to the exterior through the hyphal network constituted by the empty central parts. It favored the fossil diagenetic degradation of the hyphal network. Here, the microscopically abiotic degradation sequence of the hyphae and their surrounding amber for Spanish specimens (Fig. 7) is described. This degradation was more severe in the external parts of the amber pieces in contact with the rock matrix, providing some of the main features that the cortices show. Thus, different parts of a mycelium showed earlier and later stages of degradation depending on the distance to the external amber surface and effectiveness of the connection to the exterior through the network.

Based on SEM observations of amber cortices from Albian Peñacerrada, Salinillas, El Caleyú (Fig. 6) and San Just ambers (Fig. III), we propose a model of the sequence of hyphal degradation (Fig. 7A–D):

Stage 1 (Figs. 6A; 7A–B): in the early stage, unaltered hyphae under light microscopy show an empty central part surrounded by a hyaline wall. The contact of the wall and the amber matrix is inconspicuous as observed under SEM-SE (see Figs. 6A; IIIA–B).

Stage 2 (Fig. 7C): in this stage, holes are evident in the external surface of the wall, presenting a porous appearance (Figs. 6B–C). Depending on the state of preservation of the samples, the wall may be crossed by abundant empty radial fibrillar structures (0.1–0.3  $\mu\text{m}$ ). The absence of amber infill inside these fibrillar structures indicates that they originated after resin solidification. The presence of holes in the external surface of the wall is associated with loss of amber material located at the end of the empty radial fibrillar structures (Fig. 6B).

Stage 3 (Fig. 7D): this advanced stage of degradation can be characterized by the strong loss of wall material, mainly on its external surface, an increase in porosity and a strong loss of the surrounding amber, as can be seen with SEM-SE (Fig. 6D–F). This advanced stage implies separation of the

degraded hyphae from the amber, showing the irregularly eroded appearance of the external wall surface and the finely granulose appearance of the surrounding amber surface. Marcasite/pyrite precipitates may be present.

Most probably, marcasite/pyrite precipitates occurred during the long period of fossil diagenesis. The presence of pyrite inside amber pieces has been reported in Cretaceous and Cenozoic ambers, mainly related to bioinclusions of insects (Martínez-Delclòs *et al.*, 2004), plants and fungal mycelia (Ascaso *et al.*, 2003; Speranza *et al.*, 2010). Pyrite precipitation would have begun in the early stages of fossil diagenesis due to the anaerobic conditions in which the resin was buried. The connection from the exterior to the interior of the amber through the intricate network facilitated the precipitation of this mineral in the hyphal lumina and other empty spaces in the strongly degraded hyphae.

This model of the degradation of the hyphae can be observed, in part, in a small sample of cortex (Fig. 6), noting different grade mainly depending on the distance to the external cortex surface. However, as occurred with the non-homogeneous mineralization of nearby hyphae, it also

depends of the effective connection of the hyphae to the external chemical conditions through the lumina network (see Fig. 6C).

Some of the specimens studied by Schmidt and Schäfer (2005) showed a similar pattern of degradation, according to some of the LM and SEM photomicrographs they published. Their figure 2.2 (Schmidt and Schäfer, 2005) shows a similar degradation on the periphery of the filamentous structure. However, they interpreted these “rings of small holes” as having their origin in a supposed morphological sheath feature, the presence of granules on the outer surface, or shrinking of the sheaths during fossilization. The first explanation is at variance with another of their observations, also confirmed in the Spanish samples, which is that the resin embedded the filaments because they grew inside non-solidified resin. For us, it is clear that the SEM photomicrographs published by Schmidt and Schäfer (2005) show filaments with different degrees of degradation, ruling out the possibility that the granules on the outer surface constitute a morphological feature of the microorganism they described as a new taxon.

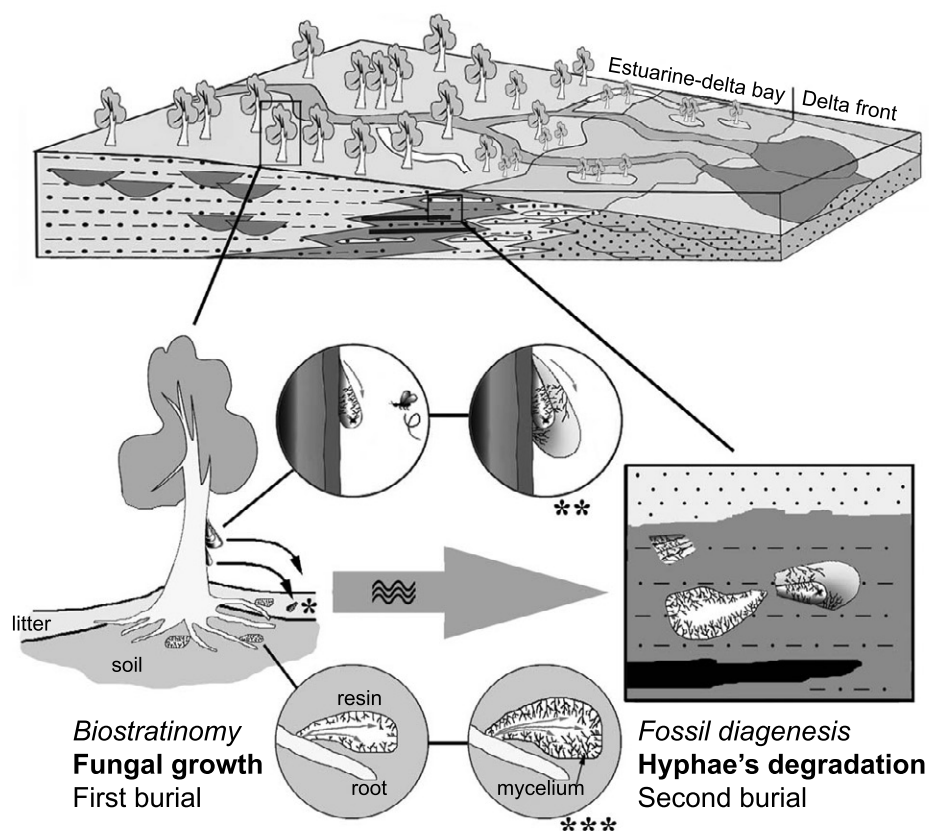


**FIGURE 8.** Schema of the main taphonomic processes in their sedimentary context showing the three scenarios inferred of the fungal growth within non-solidified resin: \* very rare (growth within aerial resin pieces fallen on the litter before complete curing of the resin), \*\* rare (growth in separated short episodes within stalactite-shaped pieces under aerial conditions), \*\*\* common (long time growth within kidney-shaped pieces under burial conditions).

Similarly, Breton and Tostain (2005) described microbubbles that sometimes extended into the amber, while others occurred inside the poorly-preserved filaments, which they interpreted as water droplets of uncertain origin. Breton and Tostain (2005) indicated that the filamentous structures from Cadeuil amber (France) were poorly-preserved and largely of the “budding hypha-like fossils” type of Waggoner (1994a). According to the descriptions of these latter authors, it seems clear that they did not consider the notable effects of degradation on the morphological features of these microorganismal filamentous structures. This degradation process explains the “dusty appearance” of the filaments and the division of the wall “into two layers, the outer one being slimmer than the inner one” described by Girard *et al.* (2009a), who did not carry out observations under SEM.

The presence of marcasite/pyrite deposits inside the lumina of some hyphae due to fossil diagenesis explains the misinterpretation of the cortices by Alonso *et al.* (2000) as alteration crusts due to their high sulfur content. Sulfur and iron content were also detected in microbiological inclusions in amber from Álava (Ascaso *et al.*, 2003; Speranza *et al.*, 2010).

#### Similar records and previous systematic assignments

The preserved polysaccharides detected ( $\beta$ -1,3 and  $\beta$ -1,4-linked polysaccharides, and *N*-acetylglucosamine residues from chitin) in the filamentous structures clearly indicated that the cortices were the result of the development of fungal mycelia. Fungal hyphae with similar sheath structures have been reported by Schönborn *et al.* (1999; see figures 33, 36 and 38), and according to these authors they are spatially related to two species of colpodid ciliates, obligate fungal feeders which are very common in terrestrial habitats worldwide.

The cortex *de visu* and microscopic morphology features published to date indicate that a similar morphotype of filamentous structures has previously been reported from diverse ambers (Poinar *et al.*, 1993; Breton and Tostain, 2005; Schmidt and Schäfer, 2005; Breton, 2007; Girard *et al.*, 2009a; Beimforde and Schmidt, 2011); the filaments show a sheathed structure very similar to the cell wall of fungal nature that has been detected using specific biomarkers.

Two Cretaceous genera and species related to this morphotype of filamentous structures have been described simultaneously from French and German amber cortices. Breton and Tostain (2005) described it as a new taxon of fossil cyanobacterium from the family Capsosiraceae, *Palaeocolteronema cenomanensis* Breton and Tostain, while Schmidt and Schäfer (2005) described it as a new

taxon of fossil sheathed bacteria (cf. Proteobacteria), *Leptotrichites resinatus* Schmidt. Nevertheless, in two subsequent collective papers (Girard *et al.*, 2009a, b), two of these authors reported that the two taxa were nearly indistinguishable on the basis of their morphology. They indicated that phycocyanin measurements can discriminate these two taxa; however, the background level of phycocyanin measured in the amber without filaments indicates a serious limitation of the technique and it was detected using destructive analyses in which all the cortex sample elements (amber and filaments) were mixed. Different results of phycocyanin measurements could originate from different degrees of fossil diagenetic preservation of the same microorganism, and modern contamination of this compound should not be ruled out due to the fact that the cortex volume is connected to the exterior through the network constituted by the empty central parts of the filamentous structures.

These identifications as bacterial groups, like others such as those of Waggoner (1994a, 1996), were originally uncertain according to the authors themselves. Waggoner (1994a) studied this morphotype of filamentous structures in amber from Bretagnolles (northwestern France) and assigned it, with reservations, to two extant cyanobacterial genera (cf. *Plectonema* and cf. *Lyngbya*). Their differences are probably due to both different degrees of degradation and mineral infillings.

Waggoner (1996) described filamentous structures with similar features in Cretaceous amber from Kansas and attributed them to sheathed bacteria closely related to the extant genus *Leptothrix*, but indicated that in the absence of biochemical and molecular analyses, such identification was tentative. Schmidt and Schäfer (2005) indicated that the micromorphological and microanalytical features of their new taxon did not correspond entirely to those of modern sheathed bacteria. Other authors (Schönborn *et al.*, 1999; Saint Martin *et al.*, 2012) have indicated that it is difficult or impossible to identify filamentous and single bacterial structures without chemical analyses. In order to avoid past and present contamination of amber pieces, biomarkers should only be directly detected on the suitable parts of the filamentous structures, using samples from amber cortices, instead of employing destructive analyses in which the sample elements are mixed. In this respect, a recent publication reported non-destructive detection of melanin compounds in hyphae from ectomycorrhizas included in amber using Raman analyses (Beimforde *et al.*, 2011).

#### Paleoecological implications

Tuovila *et al.* (2013) indicated that there is a lack of evidence of Mesozoic fungal hyphae that invaded

resin pieces and other plant exudates. For Tuovila *et al.* (2013), it suggests a late occupation of such substrates by ascomycetes, but the evidence present herein demonstrates that actually this trophic relationship is at least as old as the Cretaceous.

Breton and Tostain (2005) described *P. cenomanensis* as present in litter amber formed in terrestrial to freshwater environments in a coastal marsh; subsequently, Breton (2007) reiterated that this taxon was embedded in resin under shallow aquatic conditions in freshwater or paralic environments. Schmidt and Schäfer (2005) described *L. resinatus* as “a bacterium of limnetic habitats, probably of ponds on the forest floor of Cretaceous woodlands”. Girard *et al.* (2009a, b) interpreted the filamentous structures as bacteria trapped in resin in freshwater ponds and moist environments. In general, the above authors coincided that aquatic or sub-aquatic conditions were necessary to explain the presence of these Albo–Cenomanian fossils, in line with the taxonomical determinations provided for these fossils and other associated microorganismal inclusions.

The stalactite-shaped amber pieces from Spain (present study) and Germany (Schmidt and Schäfer, 2005) that show growths between resin flows occurring in aerial conditions, indicate that the habitat of this microorganism was not necessarily aquatic or very moist. Most probably, the microorganism inhabited the typical, variable moist conditions of tree trunks and branches and soil and litter in tropical forests. These conditions fit well with typical fungal habitats in forests. The inferred paleoenvironment of the fungus, tree trunks and roots in a humid forest, is consistent with the habitat preferences of many modern resinicolous fungi, as indicated by others (Rikkinen and Poinar, 2000, 2001).

In the Spanish amber samples with or without cortices, a plethora of protist-like inclusions (*sensu* Girard *et al.*, 2011) of diverse sizes has been observed. The presence of some putative protists that require aquatic habitats in amber pieces with cortices from other countries should be revised in the light of the general review published by Girard *et al.* (2011) regarding the frequent misinterpretation of protist-like inclusions in ambers as true protists. The new environmental scenario proposed herein, which rules out limnetic conditions for cortex formation, does not support the interpretation of those inclusions as aquatic protists. In this context, the application of biomarkers to elucidate the true protist origin of these inclusions in amber is essential.

Among the eukaryotic microorganisms, fungi, today, play a fundamental role in ecosystem processes through the decomposition of dead organic material. It is known that the production of plant resin may occur in response to fungal invasion of trunks and branches, and also in

fungal-colonized roots in extant (Singh, 1983) and extinct gymnosperms (Harper *et al.*, 2012). Although resin acts as a mechanical and/or chemical antifungal defense, several reports have suggested that it is not toxic for several soil microorganisms and can probably act as a C source in humus materials where microbes often are C-limited (Hasegawa and Takeda, 1996; Lenoir *et al.*, 1999). The introduction of a particular substrate into a soil stimulates the activity of a particular group of fungi. In this context, fungi with sufficient inoculum potential (*sensu* Garret, 1956) are able to grow in the new microhabitat, consuming said substrate. Considering the large quantity of fungal-colonized resin that can be inferred from diverse Spanish amber deposits, the inoculum potential of this resinicolous fungus in the Cretaceous forest soil seems to have been very high.

## CONCLUSIONS

The peculiar cortices constituted by networks of filamentous structures present in Spanish ambers, and by extension, ambers with similar cortices from other countries, are of biogenic, microorganismal origin. Features of both cortices and filamentous structure are uniform in the Spanish amber pieces, which indicate that only one morphotype/taxon was implicated, although a scanty presence of other taxa in the cortices should not be ruled out. We demonstrate herein that the microorganism grew inside non-solidified resin during the Cretaceous.

The molecular signature of chitin and  $\beta$ -1,3-linked polysaccharides, preserved in the walls of the filamentous structures, demonstrates that they are hyphae of resinicolous fungi. This conclusion is also supported by morphological and taphonomic evidence.

It is the first and oldest evidence of fossil fungal polysaccharides in amber, and also the first record of  $\beta$ -1,3 and  $\beta$ -1,4-linked polysaccharides, and specifically *N*-acetylglucosamine residues from chitin, in a fossil fungus. Taking into account the exceptional preservation of these fungal cell wall polysaccharides after ca. 105My, their detailed chemical characterization could be an important source of information for taxonomic and evolutionary studies.

This resinicolous fungus was a main component of the Albian resiniferous forest microcoenosis in Spain, mainly inhabiting the litter and soil and playing an important role in the recycling of organic matter, based on the abundance of strongly colonized amber pieces. Fungal proliferation in the gymnospermous resin pieces depended on the environmental conditions where the non-solidified resin occurred and/or of the fungal inoculum potential. One

important conclusion is that no aquatic or very moist conditions are necessary to explain the record of these cortices and fossil mycelia. The current available data, as yet awaiting further studies of the cortices of ambers from other countries for comparison, suggest that this conclusion is also valid at least for the Cretaceous resiniferous forests of western Laurasia.

It seems that the presence of this kind of fungus, trophically related to coniferous resins, occurred over a long geological period from the Valanginian to the Cenomanian. Its geographical distribution during the Cretaceous apparently comprised Laurasia (Spain, England, France and Germany) and North America (USA). One important question to resolve is the potential synonym for the taxa established from identical French and German cortices, *P. cenomanensis* and *L. resinatus*, which morphologically are indistinguishable from each other and also morphologically identical to the fungus described here. A review of these records should involve suitable chemical analysis in order to clearly discern their natures and their potential close relationship with the Spanish fungus, mainly focusing on the potential detection of traces of specific fungal polysaccharides using biomarkers directly on the fossil cell walls.

Several micromorphological changes occurred during the degradation sequence of the filamentous structures and the surrounding amber, as our model describes, which must be taken into account in order to conduct correct interpretations and morphological descriptions of these fossil microorganisms. The diversity of published interpretations is a consequence of the failure to integrate the taphonomic and paleoecological evidence with the ultrastructural and chemical data obtained using diverse techniques. The present research shows that it is necessary to incorporate the study of biomarkers into the list of criteria for research on microorganisms from diverse groups included in fossil resins in order to avoid misinterpretations.

#### ACKNOWLEDGMENTS

We are grateful to Dr. L. Alcalá, director of the Fundación Conjunto Paleontológico de Teruel-Dinópolis, and Mr. J. Alonso, director of the Museo de Ciencias Naturales de Álava, for giving us access to specimens and supporting part of this research, and to the landowner that permitted us to make taphonomic observations and to obtain Pleistocene samples in Waipapakauri (North Island of New Zealand). Mr. Toffa Evans (Linguistic Services of the University of Barcelona) revised the document. Especially thanks to R. López del Valle for his continuous help during the development of this research and Dr. M. Roldan, from SM-UAB for his CLSM technical assistance and discussion

on photobleaching experiments. We also extend our gratitude to Teresa Carnota (CCMA-CSIC), V. Souza-gypsi and the late F. Pinto (ICA-CSIC) for electronic microscopical technical assistance, M. Castillejo and J.M. Hontoria (MNCN) for some amber sampling preparation, A. Cortez (CAI-UCM) and A. Jorge (STND-MNCN) for CLSM technical assistance, and two anonymous reviewers, which improved the original manuscript. This study has been funded by the Diputación Foral de Álava and the grants CGL2007-62875-BOS of the former Spanish Minister of Education and Science, CGL2011-23948/BTE and CGL2014-52163 of the Spanish Minister of Economy and Competitiveness, CTM 2009-12838-CO4-03 of the former Spanish Ministry of Science and Innovation, and P631A Project by the CSIC. M.S. was contract holder of the CSIC-JAEDoc Fondo Social Europeo (Spain).

#### REFERENCES

- Allen, A.K., Neuberger, A., Sharon, N., 1973. The purification, composition and specificity of wheat germ agglutinin. *Biochemical Journal*, 131, 155-162.
- Alonso, J., Arillo, A., Barrón, E., Corral, J.C., Grimalt, J., López, J.F., López, R., Martínez-Delclòs, X., Ortuño, V., Peñalver, E., Trincão, P.R., 2000. A new fossil resin with biological inclusions in Lower Cretaceous deposits from Álava (northern Spain, Basque-Cantabrian Basin). *Journal of Paleontology*, 74, 158-178.
- Aquilina, L., Girard, V., Henin, O., Bouhnik-Le Coz, M., Vilbert, D., Perrichot, V., Néraudeau, D., 2013. Amber inorganic geochemistry: New insights into the environmental processes in a Cretaceous forest of France. *Palaeogeography, Palaeoclimatology, Palaeoecology*, 369, 220-227.
- Arcangeli, C., Yu, W., Cannistraro, S., Gratton, E., 2000. Two-photon autofluorescence microscopy and spectroscopy of Antarctic fungus: New approach for studying effects of UV-B irradiation. *Biopolymers - Biospectroscopy Section*, 57, 218-225.
- Arillo, A., 2007. Paleoethology: Fossilized behaviours in amber. *Geologica Acta*, 5(2), 159-166.
- Ascaso, C., Wierzchos, J., Corral, J.C., López, R., Alonso, J., 2003. New applications of light and electron microscopic techniques for the study of microbiological inclusions in amber. *Journal of Paleontology*, 77, 1182-1192.
- Ascaso, C., Wierzchos, J., Speranza, M., Gutiérrez, J.C., Martín-González, A., de los Ríos, A., Alonso, J., 2005. Fossil protists and fungi in amber and rock substrates. *Micropaleontology*, 51, 59-72.
- Barrón, E., Peyrot, D., Rodríguez-López, J.P., Meléndez, N., López del Valle, R., Najarro, M., Rosales, I., Comas-Rengifo, M<sup>a</sup>J., 2015. Palynology of Aptian and upper Albian (Lower Cretaceous) amber-bearing outcrops of the southern margin of the Basque-Cantabrian basin (northern Spain). *Cretaceous Research*, 52, 292-312.
- Bartnicki-Garcia, S., Persson, J., Chanzy, H., 1994. An electron microscope and electron diffraction study of the effect of

- Calcofluor and Congo red on the biosynthesis of chitin *in vitro*. Archives of Biochemistry and Biophysics, 310, 6-15.
- Beimforde, C., Schmidt, A.R., 2011. Microbes in resinous habitats: A compilation from modern and fossil resins. Advances in Stromatolite Geobiology Lecture Notes in Earth Sciences, 131, 391-407.
- Beimforde, C., Schäfer, N., Dörfelt, H., Nascimbene, P.C., Singh, H., Heinrichs, J., Reitner, J., Rana, R.S., Schmidt, A.R., 2011. Ectomycorrhizas from a Lower Eocene angiosperm forest. New Phytologist, 192, 988-996.
- Boddy, L., Frankland, J.C., Van West, P., 2008. Ecology of saprotrophic basidiomycetes. British Mycological Society Symposia Series, Academic Press, 1<sup>st</sup> edition, 386pp.
- Bowman, S.M., Free, S.J., 2006. The structure and synthesis of the fungal cell wall. BioEssays, 28, 799-808.
- Breton, G., 2007. La bioaccumulation de microorganismes dans l'ambre: analyse comparée d'un ambre céno-manien et d'un ambre sparnacien, et de leur tapis algaires et bactériens. Comptes Rendus Palevol, 6, 125-133.
- Breton, G., Tostain, F., 2005. Les microorganismes de l'ambre céno-manien d'Écommoy (Sarthe, France). Comptes Rendus Palevol, 4(1-2), 31-46.
- Briggs, D.E.G., 1999. Molecular taphonomy of animal and plant cuticles: Selective preservation and diagenesis. Philosophical Transactions of the Royal Society B: Biological Sciences, 354, 7-17.
- Burford, E.P., Kierans, M., Gadd, G.M., 2003. Geomycology: Fungi in mineral substrata. Mycologist, 17, 98-107.
- Corral, J.C., López Del Valle, R., Alonso, J., 1999. El ámbar cretácico de Álava (Cuenca Vasco-Cantábrica, norte de España). Su colecta y preparación. Estudios del Museo de Ciencias Naturales de Álava, 14, 7-21.
- Dal Corso, J., Roghi, G., Ragazzi, E., Angelini, I., Giarretta, A., Soriano, C., Delclòs, X., Jenkyns, H.C., 2013. Physico-chemical analysis of Albian (Lower Cretaceous) amber from San Just (Spain): implications for palaeoenvironmental and palaeoecological studies. Geologica Acta, 11(3), 359-370.
- Diéguez, C., Peyrot, D., Barrón, E., 2010. Floristic and vegetational changes in the Iberian Peninsula during Jurassic and Cretaceous. Review of Palaeobotany and Palynology, 162, 325-340.
- Dörfelt, H., Schmidt, A.R., Ullmann, P., Wunderlich, J., 2003. The oldest fossil myxogastroid slime mould. Mycological Research, 107, 123-126.
- Flannery, M.B., Stott, A.W., Briggs, D.E., Evershed, R.P., 2001. Chitin in the fossil record: identification and quantification of D-glucosamine. Organic Geochemistry, 32, 745-754.
- Fontaine, T., Simenel, C., Dubreucq, G., Adam, O., Delepierre, M., Lemoine, J., Vorgias, C.E., Diaquin, M., Latgé, J.P., 2000. Molecular organization of the alkali-insoluble fraction of *Aspergillus fumigatus* cell wall. Journal of Biological Chemistry, 275, 27594-27607.
- Garrett, S.D., 1956. Biology of root-infecting fungi. Cambridge, Cambridge University Press, 293pp.
- Girard, V., Néraudeau, D., Breton, G., Saint Martin, S., Saint Martin, J.P., 2008. Contamination of amber samples by Recent microorganisms and remediation evidenced by Mid-Cretaceous amber of France. Geomicrobiology Journal, 26, 21-30.
- Girard, V., Breton, G., Brient, L., Néraudeau, D., 2009a. Sheathed prokaryotic filaments, major components of Mid-Cretaceous French amber microcoenoses. Journal of Paleolimnology, 42(3), 437-447.
- Girard, V., Schmidt, A.R., Struwe, S., Perrichot, V., Breton, G., Néraudeau, D., 2009b. Taphonomy and palaeoecology of mid-Cretaceous amber-preserved microorganisms from southwestern France. Geodiversitas, 31, 153-162.
- Girard, V., Néraudeau, D., Adl, S.M., Breton, G., 2011. Protist-like inclusions in amber, as evidenced by Charentes amber. European Journal of Protistology, 47, 59-66.
- Girard, V., Breton, G., Perrichot, V., Bilotte, M., Le Loeuff, J., Nel, A., Philippe, M., Thevenard, F., 2013. The Cenomanian amber of Fourtou (Aude, Southern France): Taphonomy and palaeoecological implications. Annales de Paléontologie, 99, 301-315.
- Gonçalves, A.B., Santos, I.M., Paterson, R.R.M., Lima, N., 2006. FISH and Calcofluor staining techniques to detect in situ filamentous fungal biofilms in water. Revista Iberoamericana de Micología, 23, 194-198.
- Grimaldi, D., 2009. Did Disease Indeed Destroy the Dinosaurs? Review of: What Bugged the Dinosaurs? Death and Disease in the Cretaceous, by G. O. Poinar Jr. and R. Poinar. Princeton University Press (2008). BioScience, 59, 446-447.
- Harper, C.J., Bomfleur, B., Decombeix, A.L., Taylor, E.L., Taylor, T.N., Krings, M., 2012. Tylosis formation and fungal interactions in an Early Jurassic conifer from northern Victoria Land, Antarctica. Review of Palaeobotany and Palynology, 175, 25-31.
- Hasegawa, M., Takeda, H., 1996. Carbon and nutrient dynamics in decomposing pine needle litter in relation to fungal and faunal abundances. Pedobiologia, 40, 171-184.
- Hawksworth, D.L., Sherwood, M.A., 1981. A reassessment of three widespread resinicolous discomycetes. Canadian Journal of Botany, 59, 357-372.
- Henwood, A., 1993. Recent plant resins and the taphonomy of organisms in amber: a review. Modern Geology, 19, 35-59.
- Herth, W., Schnepf, E., 1980. The fluorochrome, Calcofluor white, binds oriented to structural polysaccharide fibrils. Protoplasma, 105, 129-133.
- Hickey, P.C., Swift, S.R., Roca, M.G., Read, N.D., 2004. Live-cell Imaging of Filamentous Fungi Using Vital Fluorescent Dyes and Confocal Microscopy. Methods in Microbiology, 34, 63-87.
- Hintikka, V., 1970. Selective effect of terpenes on wood-decomposing hymenomycetes. Karstenia, 11, 28-32.
- Hoch, H.C., Galvani, C.D., Szarowski, D.H., Turner, J.N., 2005. Two new fluorescent dyes applicable for visualization of fungal cell walls. Mycologia, 97, 580-588.

- Hoiczuk, E., Hansel, A., 2000. Cyanobacterial cell walls: News from an unusual prokaryotic envelope. *Journal of Bacteriology*, 182, 1191-1199.
- Hower, J.C., O'Keefe, J.M.K., Volk, T.J., Watt, M.A., 2010. Funginite-resinite associations in coal. *International Journal of Coal Geology*, 83, 64-72.
- Ivarsson, M., Broman, C., Holmström, S.J.M., Ahlbom, M., Lindblom, S., Holm, N.G., 2011. Putative fossilized fungi from the lithified volcanoclastic apron of Gran Canaria, Spain. *Astrobiology*, 11, 633-650.
- Ivarsson, M., Bengtson, S., Belivanova, V., Stampanoni, M., Marone, F., Tehler, A., 2012. Fossilized fungi in subseafloor Eocene basalts. *Geology*, 40, 163-166.
- Joy, D.C., 1991. An introduction to Monte Carlo simulations. *Scanning Microscopy*, 5, 329-337.
- Knight, T.K., Bingham, P.S., Grimaldi, D.A., Anderson, K., Lewis, R.D., Savrda, C.E., 2010. A new Upper Cretaceous (Santonian) amber deposit from the Eutaw Formation of eastern Alabama, USA. *Cretaceous Research*, 31, 85-93.
- Latgé, J.P., Calderone, R., 2006. The Fungal Cell Wall. In: Kües, U., Fischer, R. (eds.). *The Mycota I Growth, Differentiation and Sexuality*. Berlin, Heidelberg, Springer-Verlag, 73-104.
- Lenoir, L., Bengtsson, J., Persson, T., 1999. Effects of coniferous resin on fungal biomass and mineralisation processes in wood ant nest materials. *Biology and Fertility of Soils*, 30, 251-257.
- Lipke, P.N., Ovalle, R., 1998. Cell wall architecture in yeast: New structure and new challenges. *Journal of Bacteriology*, 180, 3735-3740.
- Maeda, H., Ishida, N., 1967. Specificity of binding of hexopyranosyl polysaccharides with fluorescent brightener. *Journal of Biochemistry*, 62, 276-278.
- Manners, D.J., Masson, A.J., Patterson, J.C., 1973a. The structure of a  $\beta$ -(1 $\rightarrow$ 3)-d-glucan from yeast cell walls. *Biochemical Journal*, 135, 19-30.
- Manners, D.J., Masson, A.J., Patterson, J.C., Björndal, H., Lindberg, B., 1973b. The structure of a beta-(1-6)-D-glucan from yeast cell walls. *Biochemical Journal*, 135, 31-36.
- Martínez, Á.T., Speranza, M., Ruiz-Dueñas, F.J., Ferreira, P., Camarero, S., Guillén, F., Martínez, M.J., Gutiérrez, A., Del Río, J.C., 2005. Biodegradation of lignocellulosics: Microbial, chemical, and enzymatic aspects of the fungal attack of lignin. *International Microbiology*, 8, 195-204.
- Martínez-Delclòs, X., Briggs, D.E., Peñalver, E., 2004. Taphonomy of insects in carbonates and amber. *Palaeogeography, Palaeoclimatology, Palaeoecology*, 203, 19-64.
- Meyberg, M., 1988. Selective staining of fungal hyphae in parasitic and symbiotic plant-fungus associations. *Histochemistry*, 88, 197-199.
- Nicole, M.R., Benhamou, N., 1991. Ultrastructural localization of chitin in cell walls of *Rigidoporus lignosus*, the white-rot fungus of rubber tree roots. *Physiological and Molecular Plant Pathology*, 39, 415-431.
- Peñalver, E., Delclòs, X., 2010. Spanish Amber. In: Penney, D. (ed.). *Biodiversity of fossils in amber from the major world deposits*. Manchester, Siri Scientific Press, 236-270.
- Peñalver, E., Delclòs, X., Soriano, C., 2007. A new rich amber outcrop with palaeobiological inclusions in the Lower Cretaceous of Spain. *Cretaceous Research*, 28, 791-802.
- Pereira, S., Zille, A., Micheletti, E., Moradas-Ferreira, P., De Philippis, R., Tamagnini, P., 2009. Complexity of cyanobacterial exopolysaccharides: Composition, structures, inducing factors and putative genes involved in their biosynthesis and assembly. *Federation of European Microbiological Societies Microbiology Reviews*, 33, 917-941.
- Poinar, G.O.Jr., 1992. *Life in amber*. California, Stanford University Press, 350pp.
- Poinar, G.O.Jr., Singer, R., 1990. Upper Eocene gilled mushroom from the Dominican Republic. *Science*, 248, 1099-1101.
- Poinar, G.O.Jr., Waggoner, B.M., Bauer, U.C., 1993. Terrestrial soft-bodied protists and other microorganisms in Triassic amber. *Science*, 259, 222-224.
- Rikkinen, J., Poinar, G., 2000. A new species of resinicolous *Chaenothecopsis* (*Mycocaliciaceae*, *Ascomycota*) from 20 million year old Bitterfeld amber, with remarks on the biology of resinicolous fungi. *Mycological Research*, 104, 7-15.
- Rikkinen, J., Poinar, G.O., 2001. Fossilised fungal mycelium from Tertiary Dominican amber. *Mycological Research*, 105, 890-896.
- Saint Martin, S., Saint Martin, J.P., Girard, V., Grosheny, D., Néraudeau, D., 2012. Filamentous micro-organisms in Upper Cretaceous amber (Martigues, France). *Cretaceous Research*, 35, 217-229.
- Schlee, D., Dietrich, H.-G., 1970. Insektenführender Bernstein aus der Unterkreide des Libanon. *Neues Jahrbuch für Geologie und Paläontologie, Monatshefte*, 40-50.
- Schmidt, A.R., Schäfer, U., 2005. *Leptotrichites resinatus* new genus and species: A fossil sheathed bacterium in alpine Cretaceous amber. *Journal of Paleontology*, 79, 175-184.
- Schönborn, W., Dörfelt, H., Foissner, W., Krienitz, L., Schäfer, U., 1999. A fossilized microcosmos in Triassic amber. *Journal of Eukaryotic Microbiology*, 46, 571-584.
- Schopf, J.W., Kudryavtsev, A.B., 2011. Confocal Laser Scanning Microscopy and Raman (and Fluorescence) Spectroscopic Imagery of Permineralized Cambrian and Neoproterozoic Fossils. In: Laffamme, M., Dornbos, S., Schiffbauer, J. (eds.). *Quantifying the Evolution of Early Life*. Amsterdam, Springer, Topics in Geobiology, 36, 241-270.
- Schopf, J.W., Kudryavtsev, A.B., Sugitani, K., Walter, M.R., 2010. Precambrian microbe-like pseudofossils: A promising solution to the problem. *Precambrian Research*, 179(1-4), 191-205.
- Schübler, A., Bonfante, P., Schnepf, E., Mollenhauer, D., Kluge, M., 1996. Characterization of the *Geosiphon pyriforme* symbiosome by affinity techniques: confocal laser scanning microscopy (CLSM) and electron microscopy. *Protoplasma*, 190, 53-67.
- Singh, P., 1983. Armillaria root rot: Influence of soil nutrients and pH on the susceptibility of conifer species to the disease. *European Journal of Forest Pathology*, 13, 92-101.

- Speranza, M., Wierzchos, J., Alonso, J., Bettucci, L., Martín-González, A., Ascaso, C., 2010. Traditional and new microscopy techniques applied to the study of microscopic fungi included in amber. In: Méndez-Vilas, A., Díaz Álvarez, J. (eds.). *Microscopy: Science, Technology, Applications and Education*. Formatex Research Center, 1135-1145.
- Stalpers, J.A., 1978. Identification of wood-inhabiting Aphyllophorales in pure culture. *Centraalbureau voor Schimmelcultures, Studies in mycology*, 16, 248pp.
- Thorn, R.G., Scholler, M., Gams, W., 2009. We accept evidence, but not conjecture, regarding fossil fungi. *Mycological Research*, 113, 276-277.
- Tuovila, H., Schmidt, A.R., Beimforde, C., Dörfelt, H., Grabenhorst, H., Rikkinen, J., 2013. Stuck in time - a new *Chaenothecopsis* species with proliferating ascomata from *Cunninghamia* resin and its fossil ancestors in European amber. *Fungal Diversity*, 58, 199-213.
- Vesentini, D., Dickinson, D.J., Murphy, R.J., 2005. The production of extracellular mucilaginous material (ECMM) in two wood-rotting basidiomycetes is affected by growth conditions. *Mycologia*, 97, 1163-1170.
- Vesentini, D., Steward, D., Singh, A.P., Ball, R., Daniel, G., Franich, R., 2007. Chitosan-mediated changes in cell wall composition, morphology and ultrastructure in two wood-inhabiting fungi. *Mycological Research*, 111, 875-890.
- Viegas, M., Martins, T.C., Seco, F., Do Carmo, A., 2007. An improved and cost-effective methodology for the reduction of autofluorescence in direct immunofluorescence studies on formalin-fixed paraffin-embedded tissues. *European Journal of Histochemistry*, 51, 59-66.
- Voigt, K., Kirk, P.M., 2011. Recent developments in the taxonomic affiliation and phylogenetic positioning of fungi: Impact in applied microbiology and environmental biotechnology. *Applied Microbiology and Biotechnology*, 90, 41-57.
- Waggoner, B.M., 1994a. An aquatic microfossil assemblage from Cenomanian amber of France. *Lethaia*, 27, 77-84.
- Waggoner, B.M., 1994b. Fossil microorganisms from Upper Cretaceous amber of Mississippi. *Review of Palaeobotany and Palynology*, 80, 75-84.
- Waggoner, B.M., 1996. Bacteria and protists from Middle Cretaceous amber of Ellsworth County. *PaleoBios*, 17, 20-26.
- Wohl, D.L., McArthur, J.V., 2001. Aquatic actinomycete fungal interactions and their effects on organic matter decomposition: a microcosm study. *Microbial Ecology*, 42, 446-457.
- Wu, B.M., Subbarao, K.V., Qin, Q.M., 2008. Nonlinear colony extension of *Sclerotinia minor* and *S. sclerotiorum*. *Mycologia*, 100, 902-910.
- Žizka, Z., Gabriel, J., 2008. Autofluorescence of the fruiting body of the fungus *Macrolepiota rhacodes*. *Folia Microbiologica*, 53, 537-539.

**Manuscript received February 2015;**

**revision accepted July 2015;**

**published Online November 2015.**

---

## ELECTRONIC APPENDIX I

---

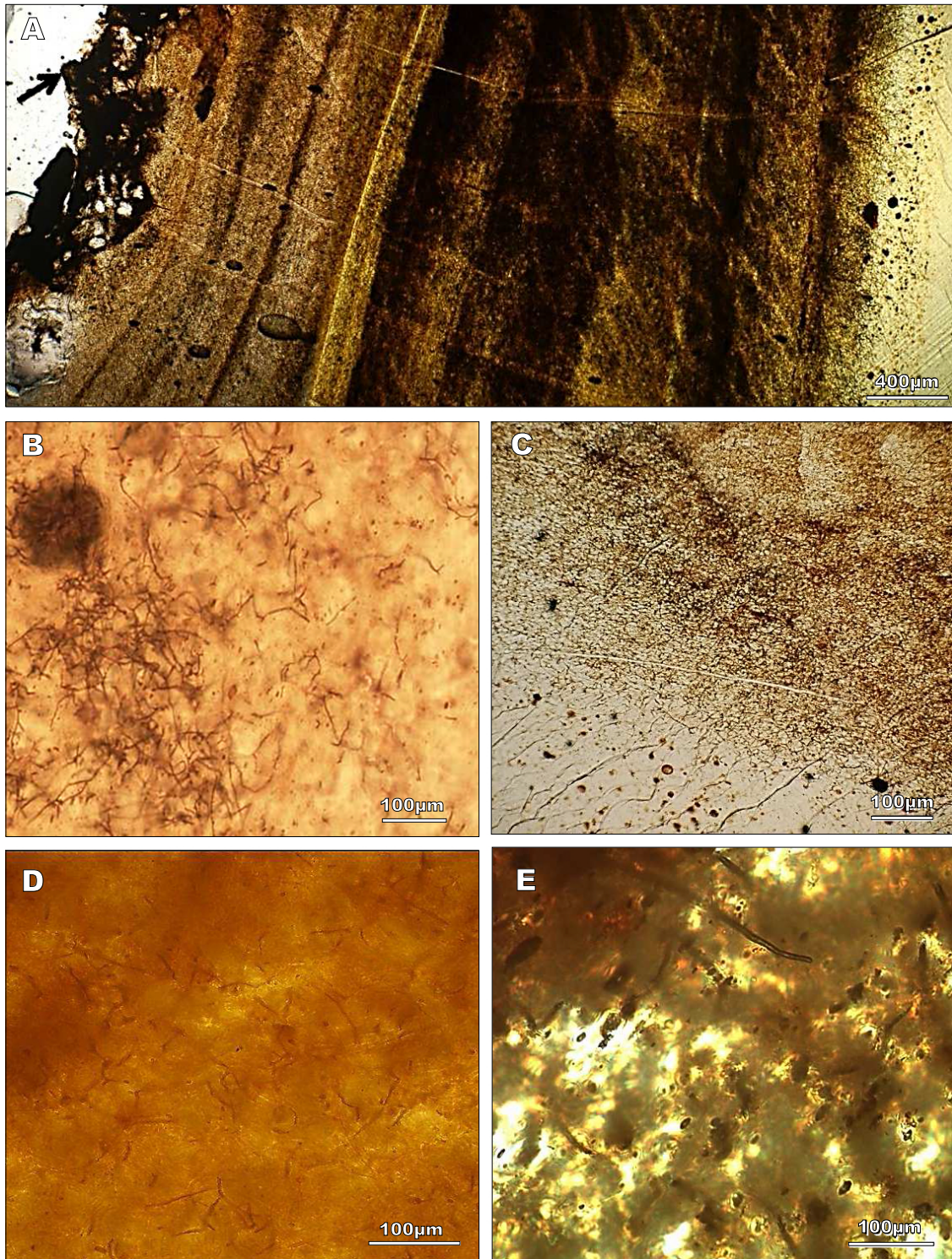


**FIGURE I.** Amber cortices light microscopy images (thin sections) from Salinillas amber. Pyrite deposits are observed in the external zone (arrow in A). Mycelium showing mineralized and non-mineralized hyphae (B–E), sparser mineralized in the internal zones (C).



**FIGURE II.** Light microscopy images of a thin section (MAP-4472) from a San Just amber cortex showing hyphae with semitransparent walls. A) Bifurcated hypha; note the halo around the lumen that constitutes the semitransparent wall. B) and E) Hyphae with walls of granulated aspect. C) Hypha with not granulated wall. D) and E) Hyphae having irregular walls due to the presence of buds and knob-like protuberances arising from their internal parts.

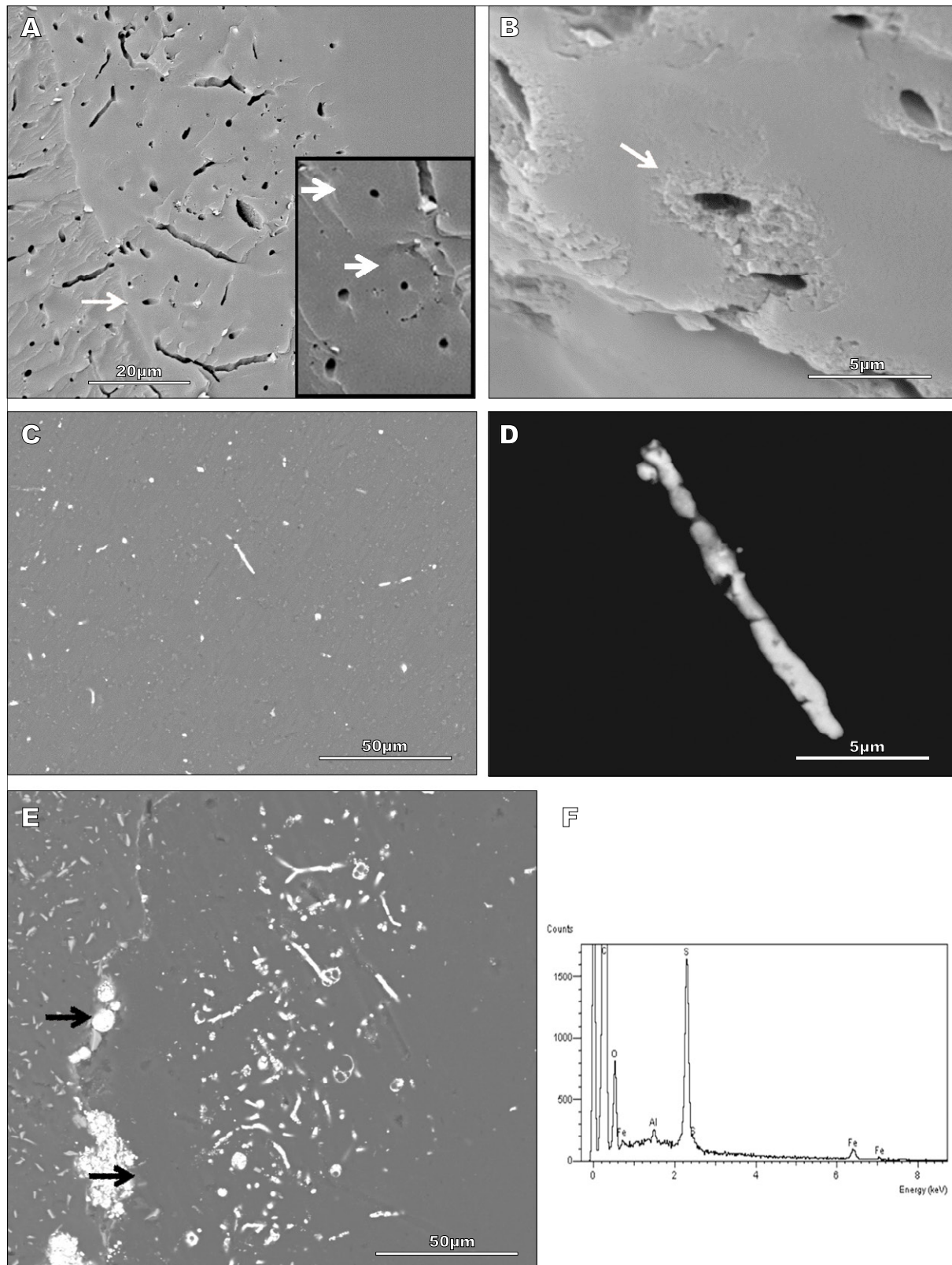


**FIGURE III.** SEM-SE and SEM-BSE images and EDS analyses of amber cortices from Salinillas de Buradón (A and B), Peñacerrada (C and D) and San Just (E) outcrops. A) and B) In non-mineralized fossil hyphae included in the amber matrix, the holes correspond to the lumen part and the limits between the halo (cell wall) of the filamentous structures and the surrounding amber could be observed (arrows). C–E) Fungal hyphae with different degree of mineralization were observed using SEM-BSE, including crystalline pyrite deposits in the external parts (arrows in E). F) EDS spectrum revealing high amount of Fe and S in the mineralized hyphae.